

**THEORETICAL HIGGS MASS BOUNDS
IN THE STANDARD MODEL
AND SUPERSYMMETRIC EXTENSIONS ***

Jose Ramón Espinosa
DESY Theory Group
Deutsches Elektronen Synchrotron DESY
22603 Hamburg, Germany

Abstract

These lectures provide a very basic introduction to different theoretical limits on the mass of Higgs scalars. Particular attention is devoted to the pure Standard Model and its Minimal Supersymmetric extension (MSSM).

* Lectures presented at the XXIV ITEP Winter School, Snegiri (Russia) February 1996.

THEORETICAL HIGGS MASS BOUNDS IN THE STANDARD MODEL AND SUPERSYMMETRIC EXTENSIONS

Jose Ramón Espinosa
DESY Theory Group
Deutsches Elektronen Synchrotron DESY
22603 Hamburg, Germany

Abstract

These lectures provide a very basic introduction to different theoretical limits on the mass of Higgs scalars. Particular attention is devoted to the pure Standard Model and its Minimal Supersymmetric extension (MSSM).

Keywords: Higgs bosons, mass bounds, Standard Model, MSSM

1. Introduction and Overview

Uncovering the elusive mechanism of electroweak symmetry breaking is one of the main goals of present and future accelerators. In these lectures I will concentrate on the most popular and simplest of all proposed mechanisms for that breaking. It makes use of a sector of fundamental scalar particles and the breaking of $SU(2) \times U(1)$ is achieved spontaneously by the vacuum expectation values (vevs) of some of these scalar fields, which have in general non-vanishing electroweak charges.

A generic prediction of these models is the existence of physical scalar particles, the Higgs bosons, remnant of the electroweak breaking searched for in accelerator experiments. The aim of these lectures is to give an introduction to some theoretical guide available for that search in the form of Higgs mass bounds. The first section starts with some general statements that can be made with the only assumption that the Higgs sector is weakly interacting. Particularly relevant examples of models, like the pure Standard Model or its minimal Supersymmetric extensions are then put in a clearer perspective by contrast with the general case.

The precise computation of an upper bound on the mass of the lightest Higgs boson in the Minimal Supersymmetric Standard Model is the topic of Section 3, while 4 and 5 are devoted to an equally precise computation of a lower bound on the Standard Model Higgs mass, from studies of the effective potential structure. These bounds lie in a mass region especially appealing for Higgs searches in the near future and are thus very relevant. Some implications that would follow from a Higgs discovery in such mass region are considered in Section 6.

2. Limits from spontaneously broken symmetries

2.1 General Sum Rules

Let $\{\phi_i\}$ be the set of Hermitian spinless fields in the theory with a potential $V(\phi_i)$ not necessarily polynomial, but invariant under some continuous symmetry G (global or local):

$$\phi_i \rightarrow \phi_i + \epsilon_\alpha \theta_{ij}^\alpha \phi_j, \quad (2.1)$$

where the θ^α 's are the generators of G , antisymmetric in our Hermitian basis.

We are interested in the case of spontaneously broken G , so that the minimum of $V(\phi_i)$ occurs at $\phi_i = \tilde{v}_i$ with $(\theta^\alpha \tilde{v})_i \neq 0$ for some of the α 's. Furthermore, we will be interested in the scalar spectrum of states in the broken minimum \tilde{v}_i . The first derivative of V with respect to the fields ϕ_i will be zero at the minimum by definition. The second derivative,

$$M_{ij}^2 = \left. \frac{\partial^2 V}{\partial \phi_i \partial \phi_j} \right|_{\phi=\tilde{v}},$$

gives the scalar mass matrix while higher order derivatives give scalar self-couplings

$$e_{ijk} = \left. \frac{\partial^3 V}{\partial \phi_i \partial \phi_j \partial \phi_k} \right|_{\phi=\tilde{v}}, \quad f_{ijkl} = \left. \frac{\partial^4 V}{\partial \phi_i \partial \phi_j \partial \phi_k \partial \phi_l} \right|_{\phi=\tilde{v}}, \dots$$

Our starting point is the invariance of the scalar potential under the transformation (2.1):

$$V(\phi_i + \epsilon_\alpha \theta_{ij}^\alpha \phi_j) = V(\phi_i) + \epsilon_\alpha \frac{\partial V}{\partial \phi_i} \theta_{ik}^\alpha \phi_k + \dots = V(\phi_i) \quad (2.2)$$

from which we obtain the identities

$$W^\alpha(\phi_i) \equiv \frac{\partial V}{\partial \phi_i} \theta_{ik}^\alpha \phi_k \equiv 0. \quad (2.3)$$

Taking derivatives of these functions W^α with respect to the ϕ_i fields and evaluating them at the minimum, relations among different parameters of the potential can be obtained. The first derivatives give

$$\frac{\partial W^\alpha}{\partial \phi_j} \equiv 0 \Rightarrow 0 = M_{ij}^2 (\theta^\alpha \tilde{v})_i, \quad (2.4)$$

which is just the familiar Goldstone's theorem: for every generator that does not annihilate the vacuum, M^2 has a zero eigenvalue. We note at this point that \tilde{v}_i can be written in general as a sum of a G -singlet s_i and a non singlet v_i . As

$\theta^\alpha \tilde{v} = \theta^\alpha v + \theta^\alpha s = \theta^\alpha v$ we will drop the tilde in the following. The second derivatives of (2.3) give a relation between masses and cubic couplings:

$$\frac{\partial^2 W^\alpha}{\partial \phi_j \partial \phi_k} \equiv 0 \Rightarrow 0 = e_{ijk}(\theta^\alpha v)_i + [M^2, \theta^\alpha]_{jk}, \quad (2.5)$$

while the third derivatives relate quartic and cubic couplings:

$$\frac{\partial^3 W^\alpha}{\partial \phi_j \partial \phi_k \partial \phi_l} \equiv 0 \Rightarrow 0 = f_{ijkl}(\theta^\alpha v)_i + e_{ijk}\theta_{il}^\alpha + e_{ikl}\theta_{ij}^\alpha + e_{ilj}\theta_{ik}^\alpha, \quad (2.6)$$

(sum over repeated indices is assumed). Now, it is simple to eliminate cubic couplings between (2.5) and (2.6) to obtain a sum rule between masses and (adimensional) quartic couplings

$$\begin{aligned} M_{ij}^2 [(\theta^\alpha \theta^\beta v)_i (\theta^\gamma \theta^\delta v)_j + (\theta^\alpha \theta^\gamma v)_i (\theta^\beta \theta^\delta v)_j + (\theta^\alpha \theta^\delta v)_i (\theta^\beta \theta^\gamma v)_j] \\ = f_{ijkl}(\theta^\alpha v)_i (\theta^\beta v)_j (\theta^\gamma v)_k (\theta^\delta v)_l. \end{aligned} \quad (2.7)$$

This is the central relation of this subsection. It implies that knowledge about the dimensionless scalar quartic couplings can be used to relate some scalar mass to the G breaking scale set by v_i , which is the only other dimensionful parameter entering (2.7). We will have occasion to see similar mass sum rules later on. Now it would be interesting to particularize (2.7) to the electroweak gauge group breaking and this example will provide a clearer picture of the relevance of (2.7).

2.1 APPLICATION: $G = SU(2)_L \times U(1)_Y \rightarrow U(1)_{em}$

There are three broken generators that we choose to be $\theta^\alpha = \{T_3, T_+, T_-\}$. Corresponding to these generators there will appear three Goldstone bosons (to be eaten by the gauge bosons). Those are given by the (complex) vectors

$$z_i = \frac{1}{N}(T_3 v)_i, \quad w_i = \frac{1}{N'}(T_- v)_i,$$

where N, N' are normalization constants related to the gauge boson masses by $M_Z = gN/\cos\theta_W$ and $M_W = gN'/\sqrt{2}$.

Conservation of electric charge implies there are only three non-trivial mass sum rules to be derived from (2.7) corresponding to the choices of $\{\theta^\alpha, \theta^\beta, \theta^\gamma, \theta^\delta\}$ with charges adding up to zero. The scalar mass matrix will have block diagonal form breaking up in different submatrices for the differently charged scalar particles. Using a mass eigenstate basis, $M_{ij}^2 = M_i^2 \delta_{ij}$ the following mass sum rules are obtained

$$\begin{aligned} f_Z &= 3 \sum_j [M_j^{(0)}]^2 A_j^2, \\ f_{ZW} &= \sum_j \left\{ [M_j^{(0)}]^2 A_j B_j + 2[M_j^{(+)}]^2 |C_j|^2 \right\}, \\ f_W &= \sum_j \left\{ 2[M_j^{(0)}]^2 B_j^2 + [M_j^{(++)}]^2 |D_j|^2 \right\} \end{aligned} \quad (2.8)$$

where $f_Z = f_{ijkl}z_i z_j z_k z_l$, $f_{ZW} = f_{ijkl}z_i z_j w_k w_l^*$, $f_W = f_{ijkl}w_i w_j^* w_k w_l^*$, are the quartic couplings of Goldstone bosons and

$$A_j = \frac{1}{N^2}(T_3^2 v)_j, \quad B_j = \frac{1}{N'^2}[(T(T+1) - T_3^2)v]_j.$$

In (2.8), superindices in mass matrices indicate the charge of the states.

Exercise. Obtain the corresponding expressions for C_j and D_j . Then prove the following relations

$$\begin{aligned} \sum_j A_j v_j &= \sum_j B_j v_j = 1, \quad A_j B_j > 0, \\ \sum_j A_j B_j &= \sum_j |C_j|^2 + \sqrt{2} \frac{G_F}{\rho^2}, \end{aligned} \tag{2.9}$$

where G_F is Fermi's constant, $(\sqrt{2}G_F)^{-1} = (246\text{GeV})^2$, and $\rho = M_W/(M_Z \cos \theta_W)$.

It is easy to transform these sum rules into useful mass inequalities. Consider the first equality in (2.8). If every (neutral) mass eigenvalue $M_j^{(0)}$ is substituted by the lowest one $M_{min}^{(0)}$ it follows that

$$3[M_{min}^{(0)}]^2 \sum_j A_j^2 \leq f_Z.$$

Furthermore, using the relations (2.9) and the Schwartz inequality, it follows

$$\sum_j A_j^2 \geq \frac{(\sum_i A_i v_i)^2}{\sum_k v_k^2} = \frac{1}{\sum_k v_k^2} \equiv \frac{1}{v^2}.$$

Then one obtains

$$[M_{min}^{(0)}]^2 \leq \frac{1}{3} f_Z v^2 \leq \frac{1}{3} f_Z (\sqrt{2}G_F)^{-1},$$

(note that possibly large singlet vacuum expectation values were dropped from the v_k 's). By similar methods the following inequalities can be obtained from (2.8):

$$[M_{min}^{(0)}]^2 \leq \left\{ \frac{f_Z}{3\sqrt{2}G_F}, \frac{f_{ZW}}{\sqrt{2}G_F} \rho^2, \frac{f_W}{2\sqrt{2}G_F} \right\}. \tag{2.10}$$

We can see explicitly here that provided the quartic couplings f are weak one expects always a scalar with mass fixed by the electroweak scale. This holds irrespective of how complicated the Higgs sector is. In the case of the minimal Standard Model, with electroweak breaking described by a single Higgs doublet, the above inequalities are the same. In fact, the inequalities are saturated and one finds the familiar

relation between the mass and quartic Higgs coupling of the Higgs boson, $M_h^2 = \lambda v^2$. In the general case there will always appear some scalar state whose mass cannot be made much bigger than the electroweak scale without making large some dimensionless coupling. It is natural to refer to that state as the 'true' Higgs boson. In general, the masses of other scalar states can instead be made heavy by choosing large values of the mass parameters in the lagrangian.

2.2 Quartic Polynomial Potentials

One remarkable property of the sum rules (2.7) obtained in the previous subsection is that the only assumption on the form of the potential was the requirement of invariance under the action of G . Then, these sum rules can be obtained even if the potential is non-polynomial (e.g. in supergravity, or in potentials including radiative corrections). However, it will prove illustrative to consider a somewhat less general situation to gain some intuitive understanding on the relation between the spontaneous breaking of some continuous symmetry and the mass limits implied by it. In this subsection we will then concentrate in cases where the potential is indeed polynomial and at most quartic in the scalar fields. From the spontaneous breaking of the symmetry G of the potential we will obtain sum rules different to those derived in the previous subsection.

Let us look more closely to the potential along the direction of the symmetry breaking. For this purpose use a mass eigenstate basis $\{\phi_A\}$. We can decompose every ϕ_A in a G -singlet part, s_A , and a non-singlet part h_A . Fixing all singlet parts to their vevs the potential for the remaining h_A -fields is trivially invariant under G . In particular, this implies that no linear terms in the h_A -fields will be allowed. Now consider the breaking direction in h_A -space. Call $\{n_A\}$ a unit vector pointing in the direction of the breaking: $n_A = \langle h_A \rangle / v$ and h the normalized field along that direction: $h = \sum_A n_A h_A$. All the G -breaking is then given by the vev of the state h , while all other orthogonal states in h_A -space will have zero vev. The potential along h can then be written in the form

$$V(h) = V(0) + \frac{1}{2}\mu^2 h^2 + \frac{1}{3}\sigma h^3 + \frac{1}{4}\lambda_h h^4, \quad (2.11)$$

The value of h at the minimum, $\langle h \rangle = v$, can be related to the parameters in the potential via the minimization conditions as usual

$$\frac{\partial V}{\partial h} = 0 \Rightarrow \mu^2 + \sigma v + \lambda_h v^2 = 0. \quad (2.12)$$

The second derivative at the minimum can be written as

$$\frac{\partial^2 V}{\partial h^2} = \sum_{A,B} n_A n_B \frac{\partial^2 V}{\partial \phi_A \partial \phi_B} = \sum_A M_A^2 n_A^2 = \mu^2 + 2\sigma v + 3\lambda_h v^2$$

or, using (2.12)

$$\sum_A M_A^2 n_A^2 = \sigma v + 2\lambda_h v^2. \quad (2.13)$$

This sum rule does not seem to be particularly useful because the right hand side contains some unknown mass parameter σ . However it is simple to see that the quantity σv is always negative in the true minimum of the potential (2.11) [the degeneracy of the two minima of (2.11) at $\sigma = 0$ is lifted by the term σh^3 . The true minimum will then correspond to $\sigma v^3 < 0$]. As a result, σv can be dropped in (2.13) to obtain the mass limit

$$\sum_A M_A^2 n_A^2 \leq 2\lambda_h v^2 \Rightarrow [M_{min}]^2 \leq 2\lambda_h v^2. \quad (2.14)$$

The last mass inequality follows the same line of Sect. 2.1 and uses $\sum n_A^2 = 1$. Note that now, the quartic coupling λ_h is not necessarily related to the Goldstone couplings that appear in the mass inequalities of (2.10) implying that in general, the mass bound (2.14) is different from those.

We can improve the previous derivation if the symmetry group G contains an $SU(2)$ subgroup (this apply in particular to the electroweak gauge group and is the reason why we concentrate on it. One can construct a similar line of derivation for any $U(1)$ subgroup of G). In that case, the Hermitian scalar fields ϕ_j will belong to some $SU(2)$ multiplet of dimension $2T_j + 1$. We can define the following parity transformation

$$P : \phi_j \rightarrow (-1)^{2T_j} \phi_j.$$

This transformation can indeed be defined for all the fields in the theory and also for products of any number of fields. Call even the fields (or product of fields) invariant under P and odd the fields that change sign under P . In particular, $SU(2)$ singlets, triplets, etc are even while doublets, quadruplets, etc are odd.

By fixing all even fields to their vevs we can obtain the potential for odd fields only. In the odd-field space we then define the normalized field

$$\varphi = \frac{1}{v_o} \sum_{odd} v_i \phi_i,$$

along the direction of the breaking. Again, all combinations of odd fields orthogonal to φ have zero vev and the potential $V(\varphi)$ must be P -invariant. Then, not only linear terms in φ are forbidden, but also cubic ones:

$$V(\varphi) = V(0) - \frac{1}{2} m^2 \varphi^2 + \frac{1}{8} \lambda_\varphi \varphi^4.$$

If φ were a mass eigenvalue it would have mass $M_\varphi^2 = \lambda_\varphi v_o^2$. In the general case it is clear that some eigenvalue will have mass below that value and the following inequality follows:

$$[M_{min}]^2 \leq \lambda_\varphi v_o^2. \quad (2.15)$$

Note that, in general, both the quartic coupling and the vev appearing in this mass bound will be different from the ones derived previously.

2.2 APPLICATION: Lightest Higgs in SUSY extended models

It is straightforward to apply the mass bound (2.15) to derive a tree level upper bound on the mass of the lightest neutral Higgs boson in general supersymmetric models. The quartic coupling for φ is obtained from two sources: F and D terms. The only terms in the superpotential that can contribute to λ_φ through F-terms will have the form $W_3 \sim h\Phi_e\Phi_o\Phi_o$ (the subindices indicate whether the chiral superfields Φ are even or odd under P). The contribution of such terms to $V(\varphi)$ will be then

$$\delta_F V(\varphi) = \frac{1}{4} \sum_i h_i^2 c_i^2 \varphi^4, \quad (2.16)$$

where the dimensionless Yukawa couplings h_i 's are in general accompanied by some rotation angles coming from the projection of the odd fields into the φ direction: $c_i = v_i/v_o$. The contribution of D-terms depends on the gauge group. Assuming the minimal $SU(2)_L \times U(1)_Y$ it is easy to obtain

$$\delta_D V(\varphi) = \frac{1}{8}(g^2 + g'^2) \left[\sum_{i, \text{odd}} Y_i c_i^2 \right]^2 \varphi^4. \quad (2.17)$$

Adding (2.16) and (2.17), eq. (2.15) gives the following mass limit

$$M_{h^0}^2 \leq (g^2 + g'^2) \left[\sum_{i, \text{odd}} Y_i c_i^2 \right]^2 v_o^2 + 2 \sum_i h_i^2 c_i^2 v_o^2. \quad (2.18)$$

In softly broken SUSY models, the details of the supersymmetry breaking do not affect the quartic couplings (at tree level) so that the scale of the mass bound (2.15) will be fixed only by the Fermi constant. As we have seen, this is not a particular feature of supersymmetric models but holds with complete generality. The Minimal Supersymmetric Standard Model has the particularity that only gauge couplings appear in (2.18). As these are measured experimentally, a well defined tree level mass bound results. In general, numerical values for the bound (2.18) can be obtained only by setting upper limits on the (unknown) h_i couplings, e.g. by triviality arguments, requiring that they remain perturbative up to some large energy scale.

Exercise. For spontaneous breaking of the electroweak gauge group: a) if driven only by $SU(2)$ doublets, show that the bounds (2.10,2.14,2.15) coincide; b) if the scalar potential has a $SU(2)$ custodial symmetry after the breaking, show that the bounds (2.10) are equal.

2.3 Interplay between different bounds and the decoupling limit

All mass bounds derived so far have in common the following property: they follow from a sum rule of the form (a simply counts different bounds)

$$\langle \varphi_a | M^2 | \phi_a \rangle = \lambda_a v_a^2, \quad (2.19)$$

where φ_a and ϕ_a are certain scalar fields [that can in general be normalized such that $\langle \varphi_a | \phi_a \rangle = 1$], M^2 is the scalar mass matrix, λ_a is some scalar quartic coupling and v_a is of the order of the breaking scale. We will call (2.19) the ‘vector-form’ of the bounds. From them, the usual ‘scalar-form’ of the mass bounds are derived straightforwardly by repeated use of $I = \sum_A |A\rangle\langle A|$, where the $|A\rangle$ are mass eigenvalues:

$$\langle \varphi_a | M^2 | \phi_a \rangle = \lambda_a v_a^2 = \sum_A \langle \varphi_a | A \rangle M_A^2 \langle A | \phi_a \rangle \geq M_h^2 \sum_A \langle \varphi_a | A \rangle \langle A | \phi_a \rangle = M_h^2.$$

In table 1 we present all five mass bounds obtained previously in vector and scalar forms. The first column gives the vectors entering (2.19). When only one vector is shown it is assumed $\varphi = \phi$. Note that only the second bound has different vectors.

Exercise. If $\langle \varphi | M^2 | \varphi \rangle \leq \lambda_\varphi v_\varphi^2$ and $\langle \phi | M^2 | \phi \rangle \leq \lambda_\phi v_\phi^2$ with $|\varphi\rangle \neq \kappa|\phi\rangle$, then $\langle \varphi | M^2 | \phi \rangle$ has also a bound of the form λv^2 . a) find λ and v^2 ; b) apply this to (2.10).

$ \phi_a\rangle, \varphi_a\rangle$	λ_a	v_a^2	$M_h^2 \leq$
$\phi_Z \sim \sum_i t_{3i}^2 v_i \phi_i$	$\frac{1}{24} \lambda_{00} (G^0)^4$	$\sum_i v_i^2$	$\frac{1}{3} \lambda_{00} v^2$
$\varphi \sim \phi_Z, \phi \sim \phi_W$	$\frac{1}{2} \lambda_{0c} G^0 G^+ ^2$	$\frac{\rho^2}{\sqrt{2}} G_F^{-1}$	$\lambda_{0c} v^2$
$\phi_W \sim \sum_i [t_i(t_i + 1) - t_{3i}^2] v_i \phi_i$	$\frac{1}{4} \lambda_{cc} G^+ ^4$	$\sum_i v_i^2$	$\frac{1}{2} \lambda_{cc} v^2$
$\frac{1}{v} \sum_i v_i \phi_i$	$\frac{1}{8} \lambda \phi^4$	$\sum_i v_i^2$	λv^2
$\frac{1}{v_o} \sum_{i, \text{odd}} v_i \phi_i$	$\frac{1}{8} \lambda_o \varphi^4$	$\sum_{i, \text{odd}} v_i^2$	$\lambda_o v_o^2$

Table 1: Summary of mass bounds.

In the following we will always assume the equality $\varphi_a = \phi_a$. The second column gives the relevant quartic couplings by showing the corresponding piece of

the scalar potential. G^0, G^\pm are the Goldstone bosons. The third column gives the values of the vev's v_i and the fourth lists the scalar form of the mass bounds.

The vector form of the bounds contains extra useful information not contained in the scalar form. As we have shown, in a particular model one can obtain several different mass bounds for the lightest Higgs scalar and by choosing the stronger among those one gets the best limit. Here we will show how the vector form can be used to extract further information on the scalar spectrum by the interplay between different bounds.

Consider the inequality

$$\sum_A \langle \phi | A \rangle M_A^2 \langle A | \phi \rangle \leq \lambda v^2.$$

If some state $|A\rangle$ is much heavier than the breaking scale, $M_A^2 \gg \lambda v^2$, its overlap with $|\phi\rangle$ has to be correspondingly small:

$$|\langle \phi | A \rangle|^2 \leq \lambda v^2 / M_A^2 \rightarrow 0.$$

This can be the case if all mass parameters in the potential are made very heavy ($\sim M$) while the pattern of symmetry breaking is held fixed (v_i constant. The required fine-tuning is bigger the heavier the mass scale M is made). We will call such situation the decoupling limit. In such limit one expects that all scalars will have masses of the order of the heavy scale $M \gg v$ with the exception of the state constrained by the mass limit λv^2 (and possibly others whose mass is protected by some symmetry). Then, if all scalars but one are very heavy, the light state $|1\rangle$ will satisfy

$$|\langle \phi | 1 \rangle|^2 = 1 - \mathcal{O}(v^2/M_A^2) \rightarrow 1.$$

This means that the state $|\phi\rangle$ appearing in the vector-form of the bound is precisely the state that will remain light in the decoupling limit.

Exercise. Given that $|1\rangle \rightarrow |\phi\rangle$ in the decoupling limit, can you prove that $M_1^2 \rightarrow \lambda v^2 = \langle \phi | M^2 | \phi \rangle$?

Suppose now that your model has two ‘linearly-independent’ bounds $\lambda_1 v_1^2 = \langle \phi_1 | M^2 | \phi_1 \rangle$ and $\lambda_2 v_2^2 = \langle \phi_2 | M^2 | \phi_2 \rangle$ with $|\phi_1\rangle \neq \kappa |\phi_2\rangle$. What would be the lightest state in the decoupling limit, $|\phi_1\rangle$ or $|\phi_2\rangle$? Of course the way out of this paradox is that the pure decoupling limit cannot be realized: at least two states will remain light:

Exercise. In the situation described above, prove that the mass of the second-to-lightest state M_2 satisfies the inequality

$$M_2^2 - M_1^2 \leq \frac{1}{\sin^2 \alpha} \left\{ \sqrt{\lambda_1 v_1^2 - M_1^2} + \sqrt{\lambda_2 v_2^2 - M_1^2} \right\}^2,$$

where α is the angle between $|\phi_1\rangle$ and $|\phi_2\rangle$.

The existence of a bound on the mass of the second to lightest scalar in such a situation can be easily understood in terms of the following geometrical construction. Consider the mass ellipsoid in the (multidimensional) scalar field space. Its axis lie along the directions of the eigenvalues with length proportional to the inverse of the corresponding squared mass eigenvalues. One mass bound of the form we have considered is given in this picture by some vector with length $(\lambda v^2)^{-1}$ and direction determined by $|\phi\rangle$. The fact that the bound is satisfied implies that the ellipsoid can at most touch the tip of this vector but cannot intersect it: $\langle\phi|M^2|\phi\rangle \leq \lambda v^2$. This is represented in the 2D example of fig. 1 a. As is clear from the picture there is necessarily an eigenvalue with mass $M_h^2 \leq \lambda v^2$. By choosing all mass parameters heavy while keeping v fixed we can flatten the ellipsoid (i.e. make the mass eigenvalues heavy) except in the vector direction of the mass bound, where the flattening is obstructed by the presence of the vector bound, that the ellipsoid cannot intersect. This is shown in fig. 1 b. From it, is clear that when all mass eigenvalues but one are heavy, the light state is given by $|\phi\rangle$. Finally, in the presence of two linearly independent mass bounds, the ellipsoid can be flattened at most to an ellipse (see fig. 1 c). The two light states, undetermined in general, will be linear combinations of $|\phi_1\rangle$ and $|\phi_2\rangle$. Obviously, this can be generalized to any number of independent mass bounds and one will expect always a number of light states in correspondence with the dimensionality of the vector space $\{|\phi_a\rangle\}$.

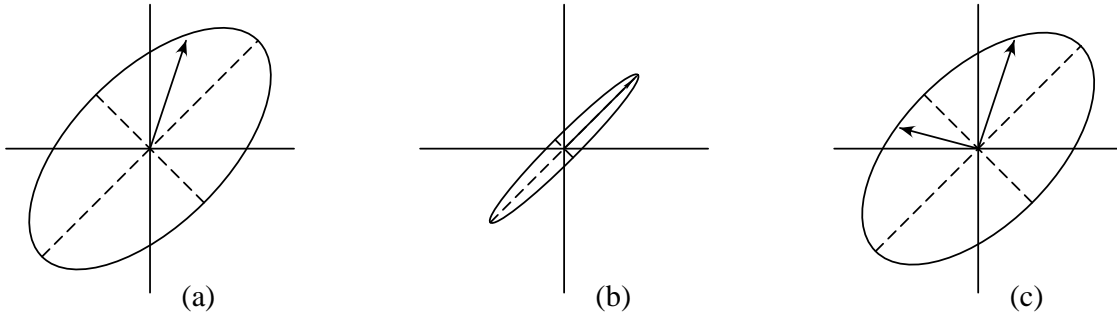


Fig. 1: Geometrical representation of the working of mass bounds.

Exercise. Suppose that there is some ‘triplet impurity’ in $SU(2)_L \times U(1)_Y$ breaking, i.e. some $SU(2)$ triplet takes a vev x and contributes to the weak vector boson masses in addition to the usual doublets. The vev x is bounded to be small by the $\Delta\rho$ constraint. In the decoupling limit, what triplet admixture do you expect in the light Higgs boson? Of which order would be the second to lightest Higgs mass?

2.2 Production Cross Section of the light Higgs boson

Concerning electroweak symmetry breaking, besides the knowledge about lim-

its on light Higgs masses one would be interested in determining whether such states can be detected experimentally at all. It is here that the information on the composition of the light Higgs becomes crucial because it determines directly the production and decay cross sections. Here we will limit ourselves as an example, to the Higgs-strahlung production mechanism of a light Higgs boson in a e^+e^- collider: $e^+e^- \rightarrow Z^* \rightarrow Zh_1$. The cross section for this process is proportional to the corresponding cross section for a Standard Model Higgs boson of the same mass. The proportionality coefficient is fixed by the gauge properties of h_1 . More precisely, the coefficient is given by the overlap between h_1 and the $|\phi_Z\rangle$ state listed in table 1:

$$|\langle\phi_Z|h_1\rangle|^2 = \frac{\sigma(e^+e^- \rightarrow Zh_1)}{\sigma(e^+e^- \rightarrow Zh_{SM})}.$$

Suppose that the model contains a scalar Higgs which is a gauge singlet. If the light state h_1 has a large overlapping with the singlet the production cross section for h_1 will be reduced. In this situation even if h_1 is forced to be below some mass bound it may be very difficult to produce and detect in accelerators. However, the important point is that from the vector form of the first bound listed in table 1 some state with a non-vanishing overlap with ϕ_Z must remain light. In other words, if the lightest Higgs turns out to be orthogonal to ϕ_Z one can still use the information from $\langle\phi_Z|M^2|\phi_Z\rangle$ to put a bound on some other Higgs. Technically this is realized in the following way: consider the quantities $\langle\phi_Z|M^2 - m_N^2|\phi_Z\rangle$, where N numbers the (scalar) Higgs mass eigenvalues, $m_1 \leq m_2 \dots$. For $N = 1$ one obtains

$$\langle\phi_Z|M^2|\phi_Z\rangle = \lambda v^2 \leq 0,$$

which is the original bound. For $N = 2$ the following inequality results

$$m_2^2 \leq \frac{\lambda v^2 - m_1^2 |\langle\phi_Z|h_1\rangle|^2}{1 - |\langle\phi_Z|h_1\rangle|^2}.$$

From this relation we see that if h_1 becomes singlet dominated $|\langle\phi_Z|h_1\rangle| \rightarrow 0$ and $m_2^2 \leq \lambda v^2$, i.e. the second to lightest eigenvalue satisfies the original bound. If on the other hand $h_1 \rightarrow \phi_Z$ then no bound on m_2 can be set. In general, for the N^{th} eigenvalue one finds

$$m_N^2 \leq \frac{\lambda v^2 - m_1^2 S_N^2}{1 - S_N^2},$$

with

$$S_N^2 = \sum_{p=1}^{N-1} |\langle\phi_Z|h_p\rangle|^2.$$

When S_N is small, for the first $N - 1$ light Higgses having reduced couplings to the Z , the bound on m_N^2 is then stronger. This effect can ensure sufficient production of some light scalar provided there are not too many singlets.

3. The lightest Higgs boson in the MSSM

3.1 The MSSM Higgs sector at tree level

Supersymmetry requires that the minimal supersymmetric extension of the Standard Model, MSSM, contains two Higgs doublets (of opposite hypercharge) to give masses to all quarks and charged leptons. The most general tree level potential for the H_1, H_2 Higgs doublets, gauge invariant and renormalizable is then:

$$\begin{aligned}
V = & m_1^2 |H_1|^2 + m_2^2 |H_2|^2 + [m_{12}^2 H_1 \cdot H_2 + h.c.] \\
& + \frac{1}{2} \lambda_1 |H_1|^4 + \frac{1}{2} \lambda_2 |H_2|^4 + \lambda_3 |H_1|^2 |H_2|^2 + \lambda_4 |H_1 \cdot H_2|^2 \\
& + \left[\frac{1}{2} \lambda_5 (H_1 \cdot H_2)^2 + \lambda_6 |H_1|^2 (H_1 \cdot H_2) + \lambda_7 |H_2|^2 (H_1 \cdot H_2) + h.c. \right],
\end{aligned} \tag{3.1}$$

with

$$H_1 = \begin{pmatrix} H_1^0 \\ H_1^- \end{pmatrix}, \quad H_2 = \begin{pmatrix} H_2^+ \\ H_2^0 \end{pmatrix}.$$

The quartic couplings in this potential are constrained by supersymmetry to be

$$\lambda_1 = \lambda_2 = \frac{1}{4}(g^2 + g'^2), \quad \lambda_3 = \frac{1}{4}(g^2 - g'^2), \quad \lambda_4 = -\frac{1}{2}g^2, \quad \lambda_5 = \lambda_6 = \lambda_7 = 0, \tag{3.2}$$

i.e. they are given in terms of the gauge coupling constants. The projection of (3.1) on the neutral Higgs components gives the potential

$$\begin{aligned}
V(H_1^0, H_2^0) = & m_1^2 |H_1^0|^2 + m_2^2 |H_2^0|^2 + [m_{12}^2 H_1^0 H_2^0 + h.c.] \\
& + \frac{1}{8}(g^2 + g'^2)(|H_1^0|^2 - |H_2^0|^2)^2.
\end{aligned} \tag{3.3}$$

The minimum of this potential determines the vevs $\langle H_1^0 \rangle = v_1/\sqrt{2}$ and $\langle H_2^0 \rangle = v_2/\sqrt{2}$ with $v_1^2 + v_2^2 = (246 \text{ GeV})^2$ fixed by the gauge boson masses. The ratio $\tan \beta = v_2/v_1$ is a free parameter. The Higgs spectrum in the broken minimum just described consists of two (CP even) scalars h^0, H^0 , one (CP odd) pseudoscalar A^0 and two charged Higgses H^\pm . Two of the three mass parameters in (3.3) can be traded by v_1 and v_2 , so that, at tree level, the properties of the Higgs sector (masses, mixing angles and couplings) are determined by one mass parameter (usually taken to be the mass of the pseudoscalar, m_A) and $\tan \beta$.

The discussion of Section 2 should have made clear that relations (3.2) have direct and important consequences for the Higgs spectrum. The tree level masses for Higgs bosons are:

$$\begin{aligned}
m_{H^\pm}^2 = & m_W^2 + m_A^2, \\
m_{h,H}^2 = & \frac{1}{2} \left[m_A^2 + m_Z^2 \mp \sqrt{(m_A^2 + m_Z^2)^2 - 4m_Z^2 m_A^2 \cos^2 2\beta} \right].
\end{aligned} \tag{3.4}$$

The two neutral Higgses are linear combinations of $H_{1,2}^{0r} \equiv \sqrt{2} \text{Re} H_{1,2}^0$, see fig. 2 :

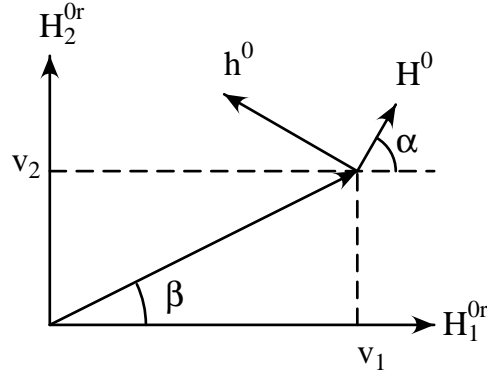


Fig. 2: Electroweak symmetry breaking in the MSSM.

$$\begin{aligned} H^0 &= (H_1^{0r} - v_1) \cos \alpha + (H_2^{0r} - v_2) \sin \alpha, \\ h^0 &= (H_2^{0r} - v_2) \cos \alpha - (H_1^{0r} - v_1) \sin \alpha, \end{aligned}$$

where the mixing angle α is given by

$$\cos 2\alpha = -\cos 2\beta \frac{m_A^2 - m_Z^2}{m_H^2 - m_h^2}, \quad \sin 2\alpha = -\sin 2\beta \frac{m_H^2 + m_h^2}{m_H^2 - m_h^2}.$$

The couplings of H^0 and h^0 relative to the Standard Model Higgs boson are then determined by α and β as shown in table 2.

	WW, ZZ	ZA	$t\bar{t}$	$b\bar{b}, \tau^+\tau^-$
h^0	$\sin(\beta - \alpha)$	$\cos(\beta - \alpha)$	$\cos \alpha / \sin \beta$	$-\sin \alpha / \cos \beta$
H^0	$\cos(\beta - \alpha)$	$\sin(\beta - \alpha)$	$\sin \alpha / \sin \beta$	$\cos \alpha / \cos \beta$

Table 2: Neutral MSSM Higgs couplings relative to the corresponding Standard Model Higgs coupling: g_{SUSY}/g_{SM} .

We can apply some of the general results examined in section 2 to the MSSM case just described. For instance, if the only mass parameter available in the Higgs sector, m_A , is made heavy (compared with the electroweak scale as given by M_Z),

eqs. (3.4) show that all Higgses will acquire masses of order m_A except one neutral Higgs that remains light, with

$$m_h^2 \leq M_Z^2 \cos^2 2\beta.$$

The inequality holds for any value of m_A and is saturated when $m_A \rightarrow \infty$. This bound explicitly derived here is the particularization to the MSSM of the general bound (2.18) and is associated with a vector $|\varphi\rangle$ in (H^0, h^0) space that lies along the direction of the breaking, see fig.2. In the decoupling limit, $m_A \gg m_Z$, we know that the light state h^0 will tend to be aligned with the vector $|\varphi\rangle$. That is, $\alpha \rightarrow \beta - \pi/2$ or

$$h^0 \sim (v_1 h_1^0 + v_2 h_2^0)/v = h_1^0 \cos \beta + h_2^0 \sin \beta. \quad (3.5)$$

In addition, a look at table 2 shows that the couplings of the light state h^0 tend to the Standard Model values in this decoupling limit. Such a Higgs scalar should be detectable then at LEP II (when $m_A \sim m_Z$ the coupling $h^0 ZZ$ can be suppressed closing the Higgs-strahlung channel but then the complimentary production mechanism $e^+e^- \rightarrow Z^* \rightarrow h^0 A^0$ becomes important).

In summary, a tree level analysis of the MSSM Higgs sector predicts the existence of a CP even Higgs scalar with mass below M_Z that should be detectable at LEP II. This would represent a stringent test for the simplest realization of the supersymmetric extension of the Standard Model. However, as is well known, the effect of radiative corrections modifies this expectation in a dramatic way.

3.2 Radiatively corrected m_{h^0} . Dominant effect

After including radiative corrections, the mass of the MSSM lightest Higgs boson is no longer determined only by m_A and $\tan \beta$ but will depend on the rest of parameters of the theory. In particular, the most important corrections come from top-stop loops that shift the squared mass of h^0 by

$$\delta m_{h^0}^2 \sim g^2 \frac{M_t^4}{M_W^2} \log \frac{M_{\tilde{t}}^2}{M_t^2}. \quad (3.6)$$

Here M_t and $M_{\tilde{t}}$ are the top and stop masses respectively. Some comments are in order. Note first that the contribution cancels if top and stops were degenerate as would correspond to the supersymmetric limit. Also note the strong dependence with M_t . As an example, if $M_t = 170 \text{ GeV}$, $M_{\tilde{t}} = 1 \text{ TeV}$, the maximum tree level value $m_{h^0} = M_Z$ would be shifted by (3.6) by as much as 30 GeV (the increase can be even more dramatic when the tree level mass is smaller).

The radiatively corrected Higgs sector of the MSSM has been intensively studied during the last years using three main tools: diagrammatic calculations, effective potential techniques and renormalization group methods. It is instructive to obtain (3.6) using these three approaches.

Exercise. Calculate the dominant correction (3.6) diagrammatically. Assume for simplicity $m_A \gg m_{h^0}$, i.e. work only with h^0 as defined in (3.5). Consider the diagrams of fig. 3 using the rules $h^0 \bar{t} t$: $H_t/\sqrt{2}$; $h^0 h^0 \tilde{t}_{L,R}^* \tilde{t}_{L,R}$: H_t^2 , where $H_t \equiv h_t \sin \beta$. Also, $M_t^2 = H_t^2 v^2/2$, $M_{\tilde{t}_L}^2 = m_Q^2 + M_t^2 + \mathcal{O}(g^2 v^2)$, $M_{\tilde{t}_R}^2 = m_U^2 + M_t^2 + \mathcal{O}(g^2 v^2)$. [Left-right mixing in the stop sector can be neglected to compute the dominant effect (3.6)].

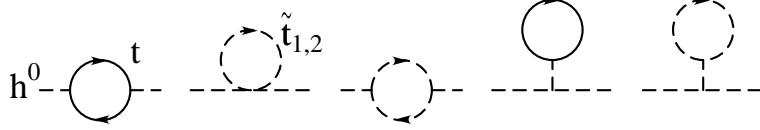


Fig. 3: Top and stop one-loop diagrams contributing to $m_{h^0}^2$.

Exercise. The one-loop MSSM effective potential when $m_A \gg m_Z$ is given by

$$V(h) = -\frac{1}{2}m^2 h^2 + \frac{1}{8}\lambda h^4 + \frac{6}{64\pi^2} \left[M_{\tilde{t}_1}^4 \left(\log \frac{M_{\tilde{t}_1}^2}{\mu^2} - \frac{3}{2} \right) + M_{\tilde{t}_2}^4 \left(\log \frac{M_{\tilde{t}_2}^2}{\mu^2} - \frac{3}{2} \right) - 2M_t^4 \left(\log \frac{M_t^2}{\mu^2} - \frac{3}{2} \right) \right],$$

with $\lambda = [(g^2 + g'^2)/4] \cos^2 2\beta$ and $M_{\tilde{t}_{1,2}}^2 = M_{\tilde{t}_{L,R}}^2$ if left-right mixing is neglected. The second derivative of the potential in the minimum $\langle \phi \rangle = v$ will give the one-loop corrected Higgs mass.

The third method, perhaps the most elegant, is based on an effective field theory approach: when the SUSY spectrum is around some scale $M_S \gg M_Z$ (in particular $M_{\tilde{t}} \sim m_A \sim M_S$) the effective theory below M_S is just the Standard Model. In particular remember that $m_A \gg M_Z$ implies that the light Higgs boson [given by (3.5)] has Standard Model-like properties. The quartic coupling of h^0 is determined by supersymmetry at the scale M_S :

$$\lambda(M_S) = \frac{1}{4}[g^2(M_S) + g'^2(M_S)] \cos^2 2\beta, \quad (3.7)$$

and its value at the electroweak scale can be computed integrating the renormalization group equations in the effective theory between M_S and the low energy scale (e.g. M_t) with (3.7) as a boundary condition. The mass of h^0 can then be obtained from λ at the weak scale by using the Standard Model relation $m_h^2 = \lambda v^2$. It is then straightforward to reinterpret the result (3.6): the logarithmic dependence arises from the running of λ from $M_{\tilde{t}} \sim M_S$ to M_t and the M_t^4 dependence comes from the dominant piece of the Standard Model beta function for λ :

$$\beta_\lambda^{SM} \sim -\frac{12}{16\pi^2} h_t^4.$$

Note that this renormalization group method is particularly well suited to study the upper bound on $m_{h^0}^2$ which is obtained in the large m_A limit.

A few comments on the structure of the radiative corrections to $m_{h^0}^2$ are in order. The fact that one-loop radiative corrections to this mass can be very sizeable (and even larger than the tree level mass if $\tan\beta$ is small) does not mean that perturbation theory is not reliable. A large ratio of one-loop corrections to tree-level contributions arises because the tree-level result does not depend on the large top Yukawa coupling while one-loop corrections do. Furthermore the one-loop result is enhanced by a logarithm of a possibly heavy mass (M_S) to a light mass (M_t). The loop contributions in the adimensional ratio $\Delta m_{h^0}^2/M_t^2$ are basically of the form

$$\sum_n \sum_{k=0}^n (\alpha \log)^k \alpha^{n-k},$$

where $\alpha = h_t^2/4\pi^2$ and $\log \sim \log(M_S^2/M_t^2)$. The terms for a given n come from the n -loop corrections, with the index k corresponding to hierarchically organized contributions (provided the log is sizeable): leading-log terms ($k = n$), next-to-leading ($k = n - 1$) and so on. For the perturbative expansion to be reliable we should require $\alpha \log < 1$ which is satisfied for the current top mass values. The use of renormalization group techniques permits to reorganize the loop expansion resumming to all loops the numerically most important corrections (leading, next-to-leading, etc). In the next subsection we discuss how to implement a computation of the loop corrected mass m_{h^0} that will include up to next-to-leading radiative corrections. Use will be made of the three methods just sketched above for the dominant correction.

3.3 Radiatively corrected m_{h^0} . Next-to-leading log computation

The ingredients for a next-to-leading log computation of the radiatively corrected m_h^0 will be discussed in this subsection. We assume that the supersymmetric spectrum can be described by a common mass M_S well above the electroweak scale. In particular $m_A \sim M_{\tilde{t}} \sim M_S$ and below M_S the effective theory is the Standard Model. As we saw, the quartic Higgs coupling at the weak scale will determine the light Higgs mass, while at the supersymmetric scale its value is fixed by supersymmetric parameters. First, we can see that the integration of the coupling λ from M_S down to the electroweak scale indeed resums some series of corrections to all loops. For example, from $d\lambda/dt = \beta_\lambda$, where $t = \log \mu$, we get

$$\begin{aligned} \lambda(M_S) - \lambda(M_t) &= \int_{\mu=M_t}^{M_S} \beta_\lambda(t) dt \\ &= \int_{\mu=M_t}^{M_S} \left[\beta_\lambda(t_0) + (t - t_0) \frac{d\beta_\lambda}{dt}(t_0) + \dots + \frac{1}{n!} (t - t_0)^n \frac{d^n \beta_\lambda}{dt^n} + \dots \right] dt. \\ &= \beta_\lambda(t_0) \log \frac{M_S}{M_t} + \frac{1}{2} \frac{d\beta_\lambda}{dt}(t_0) \left[\log \frac{M_S}{M_t} \right]^2 + \dots + \mathcal{O} \left[\log \frac{M_S}{M_t} \right]^n + \dots \end{aligned}$$

Inserting in the above expression a loop expansion for the beta function one recovers the general structure of the radiative corrections discussed at the end of the previous subsection. The one-loop approximation for the beta functions corresponds to the (all loop) leading log contributions. Using two loop beta functions would resum also the next-to-leading logs and so on.

The fact that information on higher loop corrections can be obtained with the knowledge of just one-loop beta functions is due to the magic of the Renormalization Group. Let us have a closer look to it from the point of view of the effective potential $V(\varphi)$. The starting point is the observation that a change in the renormalization scale $\mu \rightarrow \mu + d\mu$ doesn't change the physics. The invariance of the potential under such change $V(\varphi(\mu), \lambda_i(\mu); \mu) = V(\varphi(\mu + d\mu), \lambda_i(\mu + d\mu); \mu + d\mu)$, can be expressed in differential form as (sum over repeated indices implied)

$$\left[\beta_i \frac{\partial}{\partial \lambda_i} - \gamma \varphi \frac{\partial}{\partial \varphi} + \mu \frac{\partial}{\partial \mu} \right] V = 0. \quad (3.8)$$

Here λ_i stands for a generic coupling with corresponding beta function β_i , φ is the Higgs field, with anomalous dimension γ ($\gamma \varphi = -d\varphi/dt$). Note that beyond tree level the effective potential also depends explicitly on μ through logarithms. Then (3.8) connects contributions to the potential of different orders in \hbar . For example, at order \hbar^1 one has

$$\beta_i^{(1)} \frac{\partial V_0}{\partial \lambda_i} - \gamma^{(1)} \varphi \frac{\partial V_0}{\partial \varphi} + \mu \frac{\partial V_1}{\partial \mu} = 0, \quad (3.9)$$

where V_0 and V_1 are the tree-level and one loop potentials respectively and the index (1) in the β and γ functions indicate one-loop approximations. Eq. (3.9) tells that knowledge of V_0 , and one-loop rg functions allows the computation of the leading-log one-loop contribution in V_1 (which goes like $\log \mu$).

Exercise. The reciprocal is also true. From the Standard Model effective potential

$$V = -\frac{1}{2}m^2\varphi^2 + \frac{1}{8}\lambda\varphi^4 + \sum_i \frac{n_i}{64\pi^2} M_i^4(\varphi) \left[\log \frac{M_i^2(\varphi)}{\mu^2} - C_i \right],$$

with $n_t = -12$, $M_t^2 = h_t^2\varphi^2/2$; $n_W = 6$, $M_W^2 = g^2\varphi^2/4$; $n_Z = 3$, $M_Z^2 = (g^2 + g'^2)\varphi^2/4$; $n_h = 1$, $M_h^2 = 3\lambda\varphi^2/2 - m^2$; $n_\chi = 3$, $M_\chi^2 = \lambda\varphi^2/2 - m^2$ (Goldstone bosons), obtain $\beta_{m^2}^{(1)}$ and $\beta_\lambda^{(1)}$ knowing that $\gamma^{(1)} = 3[h_t^2 - (1/4)g'^2 - (3/4)g^2]$.

Defining the operators

$$\mathcal{D}^{(n)} \equiv \beta_i^{(n)} \frac{\partial}{\partial \lambda_i} - \gamma^{(n)} \varphi \frac{\partial}{\partial \varphi},$$

we can write the \hbar^2 expression of (3.8) as

$$\mathcal{D}^{(2)}V_0 + \mathcal{D}^{(1)}V_1 + \mu \frac{\partial V_2}{\partial \mu} = 0,$$

which would imply that knowledge of rg functions to two-loop order permits to obtain the leading and next-to-leading two-loop contributions in V_2 (provided V_0 and V_1 are also known).

The procedure can be extended to order \hbar^n :

$$\mathcal{D}^{(n)}V_0 + \mathcal{D}^{(n-1)}V_1 + \dots + \mathcal{D}^{(1)}V_{n-1} + \mu \frac{\partial V_n}{\partial \mu} = 0,$$

and recursion relations can be written for the n th-loop leading V_n^{LL} and next-to-leading $\log V_n^{NTLL}$ contributions:

$$\begin{aligned} \mathcal{D}^{(1)}V_{n-1}^{LL} + \mu \frac{\partial V_{n-1}^{LL}}{\partial \mu} &= 0, \\ \mathcal{D}^{(2)}V_{n-2}^{LL} + \mathcal{D}^{(1)}V_{n-1}^{NTLL} + \mu \frac{\partial V_n^{NTLL}}{\partial \mu} &= 0. \end{aligned}$$

From them we see that V_n^{LL} can be obtained from V_0 and $\mathcal{D}^{(1)}$ while to obtain V_n^{NTLL} one needs in addition V_1 and $\mathcal{D}^{(2)}$. The general statement is that the L^{th} loop potential, with parameters running with $L + 1$ rg functions resums contributions up to L^{th} -to-leading order. In our particular case we shall use the one-loop effective potential with parameters running at two-loops to resum leading and next-to-leading corrections. This should be compared with the approximation in which the tree level potential with parameters running at one-loop is used, which would resum only the leading logs.

An approximation for the effective potential truncated at some loop order, like the one we are using, will have some residual scale dependence. Understandably, this dependence will be ameliorated if we use a one-loop expression for V with two-loop running parameters as compared with the tree-level (one-loop rg improved) potential approximation. The goal is to compute reliably the second derivative of the potential (to be related with the Higgs mass) in the electroweak minimum, so that one would like to keep control on the scale dependence in that region of the minimum.

One way of doing this is the following. If the potential were known exactly it would be exactly scale independent. In such a case it is simple to show that the vev $\langle \varphi(t) \rangle$ should run with the scale in the same way as the field $\varphi(t)$ does

$$\varphi(t) = \varphi_c \exp^{-\int_0^t \gamma(t') dt'} \equiv \varphi_c \xi(t),$$

where φ_c is the classical field. Then, the ratio $\langle \varphi(t) \rangle / \xi(t)$ gives a measure of the scale independence of the potential used to extract $\langle \varphi(t) \rangle$: the ratio should be flat in the region where the potential is more scale independent. This fact can be used to determine numerically some scale t^* where indeed the above ratio turns out to

be flat. This is shown in fig. 4 , where the ratio $\langle\varphi(t)\rangle/\xi(t)$ is plotted as a function of the scale for two different approximations for the effective potential: the dashed line corresponds to the tree-level (one-loop rg improved) effective potential and the solid line to the one-loop (two-loop rg improved) case. The figure shows clearly the improvement in scale independence if the second approximation is used. The scale where the corresponding curve is flatter determines the scale t^* : not surprisingly it is of the order of the mass scale involved in the problem i.e. the top mass.

As a reassuring cross check one can also compare the real running of second derivatives (at the minimum) of the potential used with the running if the potential were scale invariant. Again it is simple to prove that $\partial^n V/\partial\varphi(t)^n$ runs like $\xi^{-n}(t)$ in the latter case. Then the ratio of $m_{h,der}^2 \equiv \partial^2 V/\partial\varphi(t)^2$ at $\langle\varphi(t)\rangle$ to $m_h^2(t) \equiv m_h^2(t^*)\xi^2(t^*)/\xi^2(t)$ measures the scale independence of the potential approximation. It turns out that this ratio becomes flatter at approximately the same scale t^* previously found which is then used as the best and most reliable scale choice for numerical computations.

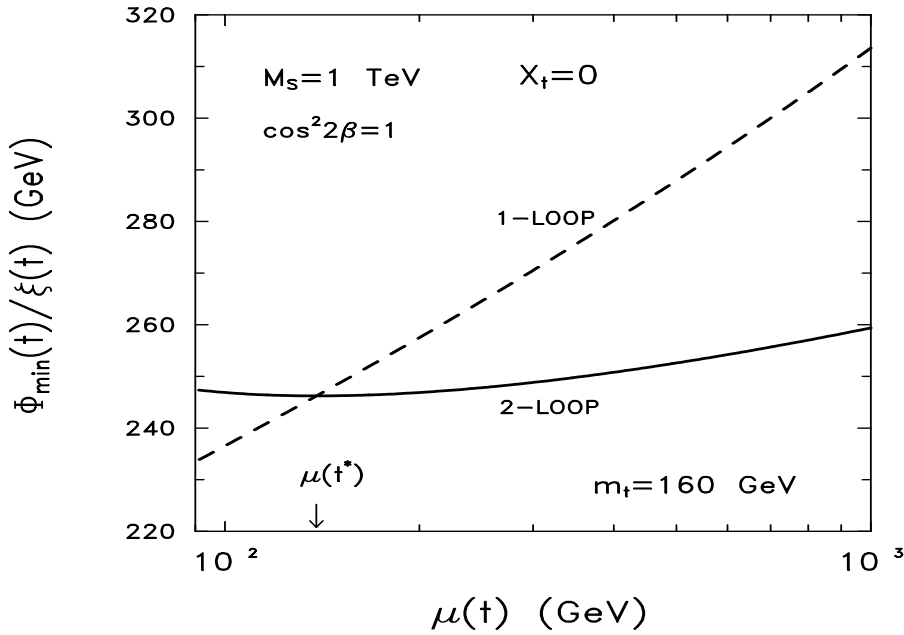


Fig. 4: Ratio $\langle\varphi(t)\rangle/\xi(t)$ as a measure of scale independence for the effective potential in two different approximations as explained in the text.

Once the scale dependence of the potential is taken care of, one can compute the second derivative at the minimum and relate it to the Higgs mass. This mass will then include logarithmic corrections up to next-to-leading order. However one should realize that this is not yet the physical mass, i.e. it does not correspond to the pole of the Higgs propagator, $\Gamma_R(p^2) = p^2 - (m_R^2 + \Pi_R(p^2))$, where p is the external momentum, m_R is the renormalized mass and Π_R the one-loop self-energy.

Remembering that the effective potential generates 1PI diagrams with *zero* external momentum we get

$$m_h^2(t) \equiv \left. \frac{\partial^2 V}{\partial \varphi^2} \right|_{\langle \varphi \rangle} = -\Gamma_R(p^2 = 0) = m_R^2 + \Pi_R(0).$$

The pole mass being defined by $\Gamma_R(p^2 = M_H^2) = 0$, we arrive at

$$M_H^2 = m_h^2(t) + \Pi_R(p^2 = M_H^2) - \Pi_R(p^2 = 0). \quad (3.10)$$

It can be shown that the scale dependence of $m_h^2(t)$ cancels at one-loop with the self-energy difference correction giving rise to a pole mass scale independent up to higher orders. The diagrammatic calculation of the one-loop self-energies adds to the Higgs mass the one-loop corrections not accessible to rg resummation. A similar self-energy correction should be included to relate the running top mass $m_t(t) = h_t(t)v\xi(t)/\sqrt{2}$ with the top pole mass M_t . The dominant piece comes from QCD radiative corrections. In $\overline{\text{MS}}$ it reads

$$M_t = m_t(\mu = M_t) \left[1 + \frac{4}{3} \frac{\alpha_s(M_t)}{\pi} \right]. \quad (3.11)$$

The last piece for a consistent computation of m_{h^0} at next-to-leading order corresponds to the inclusion of one-loop threshold corrections to the boundary condition (3.7). They arise when integrating out the heavy supersymmetric particles. The dominant contribution corresponds to stops and is represented diagrammatically in fig. 5 . It is a simple **Exercise** to compute it either by expanding the contribution of stops to the MSSM potential in powers of the background Higgs field or by diagrammatic calculation. The correction to $\lambda(M_S)$ is proportional to the stop mixing $M_{\tilde{t}_L \tilde{t}_R}^2 = H_t \varphi X_t$, where $H_t = h_t \sin \beta$ and $X_t = (A_t + \mu \cot \beta)$:

$$\delta\lambda = \frac{3H_t^4 X_t^2}{8\pi^2 M_S^2} \left[1 - \frac{X_t^2}{12M_S^2} \right]. \quad (3.12)$$

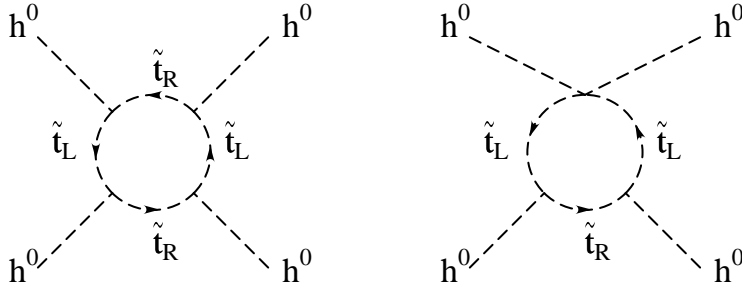


Fig. 5: Two types of supersymmetric diagrams giving the dominant threshold corrections to the quartic Higgs coupling.

The shift in λ reaches a maximum value for $X_t^2 = 6M_S^2$ that corresponds then to the maximum of the Higgs mass (maximal mixing case). The case of negligible mixing $X_t \sim 0$ (minimal mixing case) will in general correspond to the minimum value of the Higgs mass (when the rest of parameters is fixed). Note that the correction (3.12) can be negative if $X_t^2 > 12M_S^2$. However in that region of parameters is easy to run into problems with color or charge breaking minima in the full supersymmetric scalar potential.

This completes the list of ingredients for the next-to-leading log computation of m_{h^0} . An example of the results is plotted in fig. 6 which gives the (physical) Higgs mass versus the (pole) top mass.

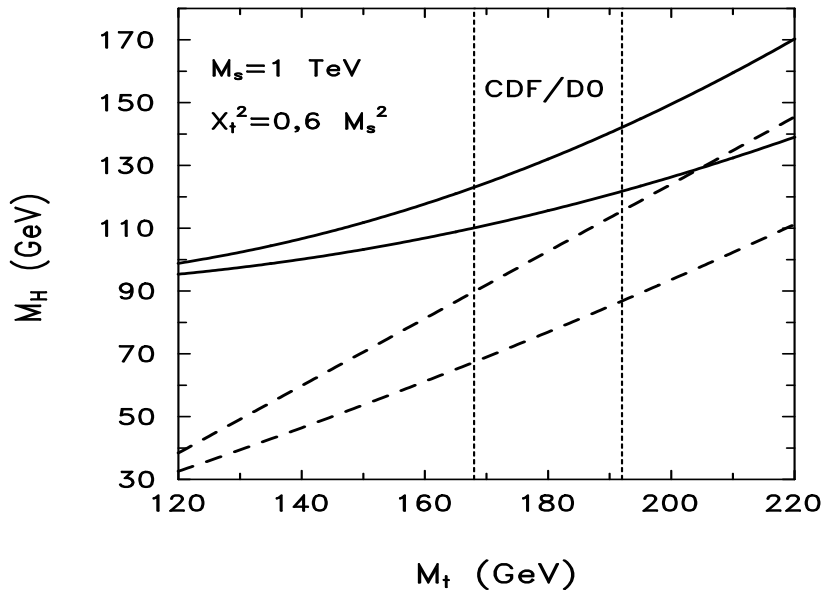


Fig. 6: Upper limits for the lightest Higgs boson in the MSSM with the scale of supersymmetry $M_S = 1 \text{ TeV}$. Solid lines: $\tan \beta \gg 1$, dashed lines: $\tan \beta = 1$. For a given $\tan \beta$ the upper (lower) curve corresponds to $X_t^2 = 6M_S^2$ ($X_t = 0$).

The scale of the supersymmetric particles is set to 1 TeV which is roughly the upper limit from naturalness arguments. As the pseudoscalar mass m_A is then much larger than the electroweak scale, the masses shown in the figure are actually the upper limits for m_{h^0} (for the corresponding value of M_S). The masses do increase logarithmically with M_S . Solid lines correspond to the case of large $\tan \beta$ while dashed lines have $\tan \beta = 1$. In each pair, the upper curve is the one for maximal mixing $X_t^2 = 6M_S^2$ (giving then the absolute bound on m_{h^0}) and the lower for the minimal mixing case $X_t \sim 0$. Short-dashed vertical lines give the CDF/D0 range for the top mass. From the figure is clear that LEP II can miss the lightest Higgs boson if e.g. $\tan \beta$ turns out to be large and stops are heavy with substantial mixing.

A few comments are in order before closing this section. When there is still a hierarchy between M_S and M_t but $m_A \sim M_t$ one can repeat the above procedure with the difference that now, the effective theory below M_S is a two Higgs doublet extension of the Standard Model. The Higgs potential is then that written in (3.1) with quartic couplings fixed by supersymmetry at the scale M_S . The `rg` program uses now `rg` functions for the two Higgs doublet model to evolve the mass matrix for neutral scalars, plus the masses for charged Higgs bosons from M_S down to the electroweak scale. The mass of the lightest Higgs boson is smaller in this case.

The fact that a clever choice of the renormalization scale permits to obtain reliable results in a leading log calculation can be used to derive simple analytical formulas for radiatively corrected Higgs masses (and couplings). This can be done by iteratively integrating `rg` equations to the required precision.

4. Standard Model Stability Bound on the Higgs Mass

In section 3 we saw that in the MSSM large radiative corrections to the lightest (CP even) Higgs mass arise in the case of a heavy supersymmetric scale. By using effective theory methods, the corrections were described as a renormalization group effect: the quartic Higgs coupling at the supersymmetric scale is small (as it is fixed by electroweak gauge couplings) but is driven to large values at the electroweak scale by the top quark contributions to $\beta_\lambda \sim -12h_t^4/(16\pi^2)$ which dominate the running of λ if the top is heavy.

This effect of top loop corrections is a purely Standard Model effect (the running of λ below the supersymmetric scale is described by the Standard Model `rg` functions) and has interesting consequences already in the pure Standard Model. The steepness in the running of λ implies that if this quartic coupling is small at the electroweak scale (this means a light Higgs mass) it can be driven to negative values at a large scale if the top is sufficiently heavy. A negative value of λ signals the appearance of an instability in the effective potential at large values of the field: $V(\varphi) \sim \lambda\varphi^4 \rightarrow -\infty$. If this pathology would appear for values of the field well beyond the Planck mass we shouldn't worry about it because we know already that the Standard Model has to be modified at such energy scales. In general, if the Standard Model is valid up to some large energy scale Λ (where some new physics will take over) we should be concerned about the possibility that the effective potential is destabilized below Λ . To avoid this pathology the Higgs mass should be heavy enough

$$M_H > M_H^c(M_t, \Lambda),$$

where the critical value M_H^c will be a monotonically increasing function of the top mass (the heavier the top is, the steeper the descent of λ will be) and the scale Λ (the larger Λ is, the longer will be the running of λ). The interesting point is that, for the current CDF/D0 values of the top mass the limits M_H^c are around 100 GeV, a region with direct significance for future Higgs searches. It would then

be desirable to compute these critical masses, dubbed stability bounds, with good precision and this can be done following a procedure very similar to the one used in the previous section to compute the upper bound for the lightest MSSM Higgs boson mass.

Before that, let us have a closer look at the instability of the potential. We need to compute reliably the value of the effective potential at large values of the field to see whether it is below the value at the electroweak minimum, in which case this minimum would get destabilized and eventually decay. As we don't know the exact potential we have to rely in perturbative approximations and so, a convenient choice of the renormalization scale should be made. To start just consider the choice $\mu \sim M_Z$ that has the advantage that we know the values of the couplings without having to run them. The tree level potential is just

$$V_0(\varphi) = -\frac{1}{2}m^2\varphi^2 + \frac{1}{8}\lambda\varphi^4,$$

with $\lambda(M_Z)$ obviously positive, so that no instability would arise at high φ . If we add one-loop corrections we discover that the dominant piece comes from top loops [see fig. 7 (a)] and is

$$\Delta V_1 = \sum_i \frac{n_i}{64\pi^2} M_i^4(\varphi) \left[\log \frac{M_i^2(\varphi)}{\mu^2} - C_i \right] \simeq -\frac{12}{64\pi^2} \frac{1}{4} h_t^4 \varphi^4 \left[\log \frac{h_t^2 \varphi^2}{2\mu^2} - \frac{3}{2} \right]. \quad (4.1)$$

[Here n_i counts the number of degrees of freedom of the i^{th} particle with field-dependent mass $M_i^2 = \kappa_i^2 \varphi^2$ (this form for the masses holds for the main contributions to the potential. Higgs bosons have an additional field-independent piece, but their contribution is not important numerically). C_i are some numerical constants.] We see that, for sufficiently large values of φ this piece dominates over the tree-level part and being negative drives the potential to negative values. Once again, the fact that ΔV_1 dominates over V_0 does not imply that the perturbative expansion is not well behaved. In a similar way as what we discussed in the previous section the expansion parameter is of the form $\alpha \log$ where again $\alpha \sim h_t^2/16\pi^2$ and now $\log \sim \log(\phi/\mu)$. To be confident that the instability is really there, it has to appear for values of the field where $\alpha \log < 1$. The fact that this can actually happen is then a consequence of the hierarchy $h_t \gg \lambda$ of the relevant coupling in the loop correction to the relevant coupling in the tree level potential. On the other hand note that the log depends now on the scale μ . This means that fixing $\mu \sim M_Z$ we cannot reliably study potential instabilities if they appear at field values much larger than $\varphi \sim M_Z \exp(4\pi)$. Assuming this is not the case, if $\alpha \log < 1$ but not too small one should care about higher order corrections. For example the dominant two-loop correction to the potential (at large φ) has the form

$$\Delta V_2(\varphi) \simeq \frac{h_t^4}{(16\pi^2)^2} \left[\# \left(\log \frac{h_t^2 \varphi^2}{2\mu^2} \right)^2 + \# \left(\log \frac{h_t^2 \varphi^2}{2\mu^2} \right) + \# \right], \quad (4.2)$$

where the $\#$'s are field independent constants (some combination of couplings) [the dominant diagrams are depicted in Fig. 7 (b,c)].

Exercise Taking advantage of the scale invariance of the effective potential compute the value of the constant $\#$ for the two-loop leading log contribution in (4.2) (keeping only h_t and g_S couplings). Use the knowledge of ΔV_1 and the one-loop rg functions $16\pi^2\gamma^{(1)} \simeq 3h_t^2$ and $16\pi^2\beta_{h_t}^{(1)} \simeq h_t[(9/2)h_t^2 - 8g_s^2]$.

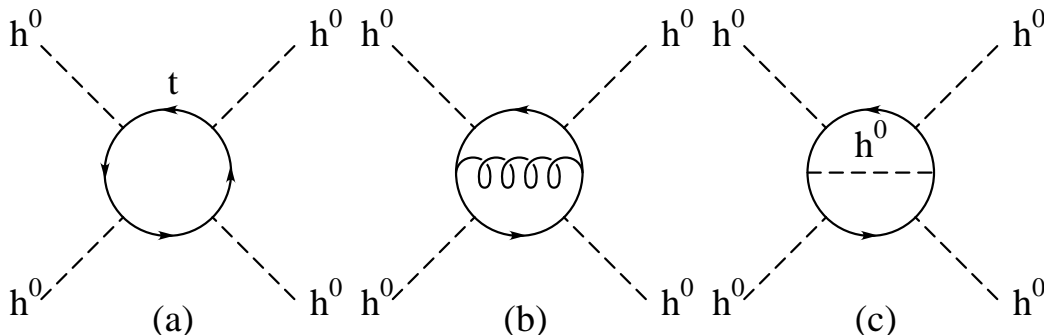


Fig. 7: Dominant loop diagrams contributing to the running of λ . (a) One-loop and (b,c) two-loops .

From the previous discussion it is clear that we can use our freedom in choosing μ to have a reliable perturbative expansion by the choice $\mu \sim \varphi$. This choice will make small the radiative corrections so that we can just work with the tree level potential. Of course, this doesn't mean that the destabilization disappears (being caused by large loop corrections). The size of radiative corrections is scale dependent and only the full potential doesn't depend on the scale. By choosing $\mu \sim \varphi$ we just reorganize the expansion in such a way that the bulk of the effect is transferred from the higher loop corrections to the tree level part. The instability appears then as a result of $\lambda(\mu \sim \varphi) < 0$. We have then a clear picture of the procedure to follow: we consider the tree-level effective potential with parameters evaluated at some scale μ . When $\lambda(\mu)$ runs to negative values, it means that the potential is being destabilized at φ of that order. Imposing that this destabilization scale is larger than the cut-off scale Λ we can compute the stability bound for that Λ : the lowest allowed value for $\lambda(\mu \sim M_Z)$ (and thus for M_H) is such that $\lambda(\mu \sim \Lambda) = 0$ (which is in practice used as a boundary condition for the running λ). Implementing that program with one-loop rg functions amounts to compute the stability bound at leading-log order.

For large Λ (say $\Lambda \sim M_{Pl}$) the leading-log calculation can be a good enough approximation for the stability bound. A better precision can be achieved with a next-to-leading log calculation, proceeding along similar lines as what was done in section 3. Understandably, the NTLL calculation is mandatory in the case of lower Λ , say $1 - 10 TeV$, when the effect of NTLL terms can become more important.

The ingredients for a NTLL calculation should be clear by now. First, use a one-loop effective potential with parameters running with two-loop rg functions.

Next, keep control of the scale dependence of the potential. This has to be done in two regions of φ : in the region near the electroweak minimum, to ensure that the potential is minimized properly and the Higgs mass extracted correctly (as was done in the previous section) and then, in the region of the instability. In that region one can fix $\mu = \alpha\varphi$ and study the flatness of the bounds with the parameter α . Again, it turns out that, the tree-level calculation of the bound requires a careful choice of the scale while the one-loop calculation is much more stable.

As a result of using a one-loop expression for the potential, one should replace the boundary condition $\lambda(\Lambda) = 0$ by a one-loop corrected version of it $\tilde{\lambda}(\Lambda) = 0$. Here $\tilde{\lambda}$ is basically the one-loop coefficient of φ^4 (once $\mu = \alpha\varphi$). From (4.1)

$$\tilde{\lambda} \simeq \lambda + \sum_i \frac{n_i}{8\pi^2} \kappa_i^2 \left[\log \frac{\kappa_i^2}{\alpha^2} - C_i \right].$$

The fact that $\tilde{\lambda}$ should be used for a faithful description of the potential destabilization is exemplified by fig. 8. For the indicated values of the parameters, the first plot gives the behaviour of the potential. Note the appearance of a deep non-standard minimum at large values of the field. The second is a plot of the running of λ and $\tilde{\lambda}$ with the scale, showing that the scale of destabilization of the potential indeed coincides with the scale at which $\tilde{\lambda}$ crosses zero. The point where λ is zero is instead an order of magnitude lower.

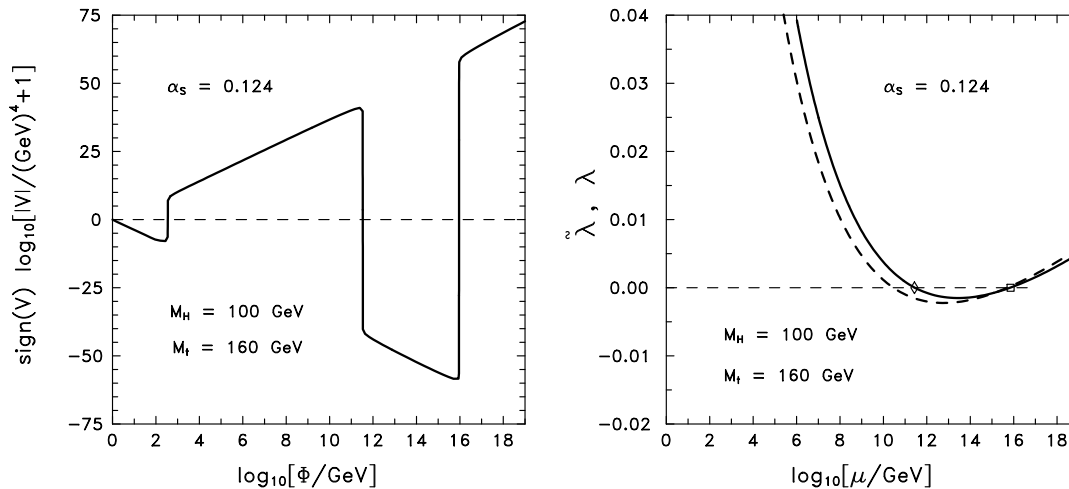


Fig. 8: Right: Effective potential. Left: Running λ (dashed) and $\tilde{\lambda}$ (solid).

Note that the potential does not run to $-\infty$ for large field values but rather turns again to positive values. This is caused by the decrease of h_t at high scales.

The destabilizing force then weakens and eventually the effect of gauge couplings takes over making the couplings λ and $\tilde{\lambda}$ positive again (see left plot in Fig. 8).

The last ingredient for the NTLL computation of the bound is to extract physical masses for M_H and M_t as explained in Section 3 [Eqs. (3.10) and (3.11)]. The NTLL results are typically $\mathcal{O}(10)$ GeV lower than the LL ones and even more [$\mathcal{O}(20)$ GeV] for low cut-offs [e.g. $\Lambda \sim 10^3$ GeV]. The bounds, as a function of M_t and Λ are plotted in fig. 9 . There is a non-negligible dependence on α_s (larger for larger Λ) the bound being larger for smaller α_s .

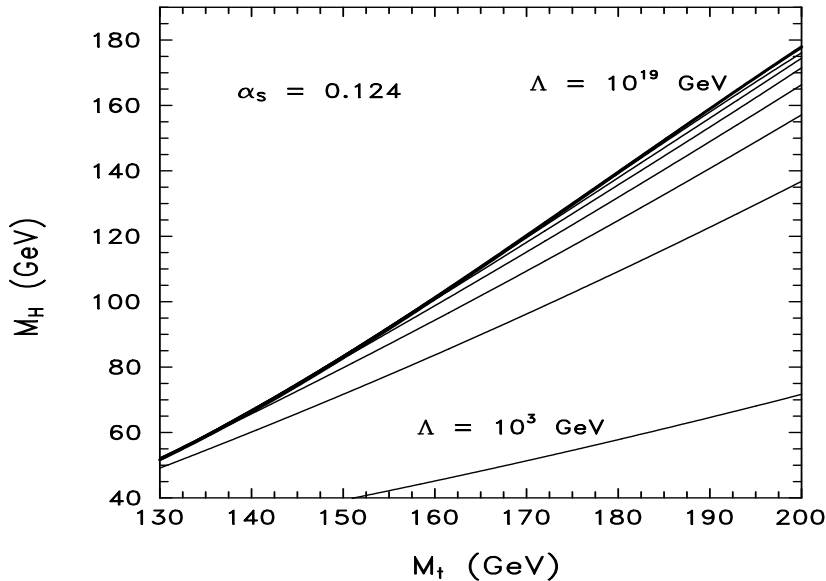


Fig. 9: Stability bounds for the Standard Model Higgs mass as a function of the top mass M_t and the cut-off scale Λ from $\Lambda = 10^3$ GeV to 10^{19} GeV in steps of two orders of magnitude.

The area below a given curve corresponds to a region of parameters where the effective potential develops an instability at field values below the corresponding cut-off. This cut-off is usually referred to as the scale of new physics and should be interpreted with some care. The correct way of thinking about it is that, for a given pair (M_t, M_h) in the instability area, there is a curve labeled by some value of Λ that goes through that point. That value of Λ is the scale at which the instability develops in the pure Standard Model for the specified values of M_t and M_h . As such, it can be computed very precisely, irrespective of whether Λ is large or small. In case that for the experimental value (M_t, M_h) the instability scale $\Lambda(M_t, M_h)$ is below the Planck mass it would imply that the Standard Model would have to be extended in such a way that the instability is cured. This means that new physics should have an effect at scales below Λ .

5. Standard Model Metastability Bound on the Higgs Mass

Strictly speaking, we may admit the possibility that the electroweak vacuum is not the deepest vacuum of the effective potential provided it is sufficiently long lived and the decay probability to the true vacuum is negligible. In the presence of a large potential barrier separating the two vacua it is reasonable to expect that the decay rate for tunneling (per unit time and unit volume) would be exponentially suppressed. However the Universe is old and large and it turns out that for some choices of the parameters below the stability curve (e.g. for $M_t = 180 \text{ GeV}$ and $M_h = 100 \text{ GeV}$) the unstable electroweak vacuum should have decayed long ago and are thus unacceptable if no new physics is at work at (or below) the scale of the instability. Then, the requirement that an unstable vacuum is acceptable if its lifetime is longer than the age of the Universe weakens the stability bounds derived in the previous section increasing the allowed range of Higgs masses.

However, there is a more stringent requirement an unstable electroweak vacuum should meet: it has to survive the high temperatures in the early Universe, when thermal excitations can trigger the decay to the true vacuum. The Higgs potential in the presence of the thermal plasma in the early Universe depends strongly on the temperature, T . For T much larger than the scale of instability, Λ , $SU(2) \times U(1)$ symmetry is restored and the only minimum of the potential is at the origin. At $T \sim \Lambda$ a new local minimum appears at a scale $\phi \sim T \sim \Lambda$ and at some temperature T_c^1 the new minimum becomes degenerate with the one at the origin. For $T < T_c^1$ the minimum away from the origin is the deepest and the decay from the minimum at the origin to it becomes possible. For lower and lower temperatures the true minimum gets deeper and deeper evolving to the non-standard $T = 0$ vacuum at $T \ll \Lambda$. The barrier between the two vacua is always present. Eventually, if the Universe remains trapped at the origin, at a temperature T_c^{EW} of order 100 GeV the standard electroweak phase transition takes place, $SU(2) \times U(1)$ gets broken and the Universe sits in a new minimum that lies at the electroweak scale. The possibility of a no-return transition to the non-standard minimum is more likely than tunneling from quantum fluctuations at $T = 0$. For example, if $M_t = 180 \text{ GeV}$ and $M_h = 130 \text{ GeV}$, the unstable electroweak vacuum would be safe against quantum tunneling but cannot survive the high temperature early Universe.

The phase transition to the non-standard minimum is strongly first order and proceeds via thermal nucleation of bubbles of true phase that grow till they fill the Universe. If a bubble of true phase is too small it collapses under surface tension while, if it is large enough the gain in potential energy compensates surface tension and the bubble grows. There is then a critical bubble, a saddle point of the free energy functional, that gives the critical energy that appears in the Boltzmann exponent for the decay rate. Consider a static and spherically symmetric bubble of true vacuum with Higgs profile $\phi(r)$. Here r is spatial distance from the center of the bubble, so that $\phi(0)$ probes the instability region of the potential and $\phi(r \rightarrow \infty)$ goes to the false vacuum. At a given temperature, the extra energy for such a

configuration in a sea of false vacuum is given by

$$E[\phi(r)] = 4\pi \int_0^\infty r^2 dr \left[\frac{1}{2} \left(\frac{d\phi}{dr} \right)^2 + V(\phi, T) - V(v_{false}, T) \right].$$

The critical bubble minimizes this energy and so the critical bubble profile is the solution of the Lagrange equation

$$\frac{d^2\phi}{dr^2} + \frac{2}{r} \frac{d\phi}{dr} = \frac{dV}{d\phi},$$

with boundary conditions

$$\phi(r \rightarrow \infty) = v_{false}(T), \quad d\phi/dr|_{r=0} = 0.$$

Here $v_{false}(T)$ is the field expectation value in the minimum close to the origin: $v_{false} = 0$ for $T > T_c^{EW}$ and $v_{false} = v_{EW}(T)$ for $T < T_c^{EW}$. For a given temperature T , the effective potential is known and the critical bubble profile $\phi_B(r)$ and energy $E_B(T) = E[\phi_B(r)]$ can be computed. The rate of nucleation of these bubbles per unit time and unit volume is then given by

$$\Gamma/\nu \sim \omega T^4 \exp[-E_B(T)/T], \quad (5.1)$$

with ω a constant that can be taken of order unity for our purpose. The qualitative dependence of E_B with temperature is shown in fig. 10. For Higgs masses larger than the LEP I experimental bound $\sim 65 \text{ GeV}$ the deepest minimum of the curve appears always in the region $T \gg T_c^{EW}$ so that the decay rate is maximal at temperatures much larger than T_c^{EW} .

To get the probability of decay, the rate (5.1) should be multiplied by the volume of our current horizon scaled back to temperature T . The differential probability is then

$$\frac{dP}{d \log T} = \kappa \frac{M_{Pl}}{T} \exp(-E_B/T),$$

with $\kappa \sim 3.25 \times 10^{86}$ and is plotted also in fig. 10. Obviously it peaks near the minimum of E_B/T . The integrated probability of decay is then

$$P = \int_0^{T_c^1} \frac{dP(T')}{dT'} dT'. \quad (5.2)$$

Note that this probability is not normalized to one. In fact its interpretation is that the fraction of space that remains in the old metastable phase is given by $\exp(-P)$. So, $P \gg 1$ (see fig. 11) indicates that the metastable electroweak vacuum would have decayed to the non-standard minimum in the hot early epoch of the Universe.

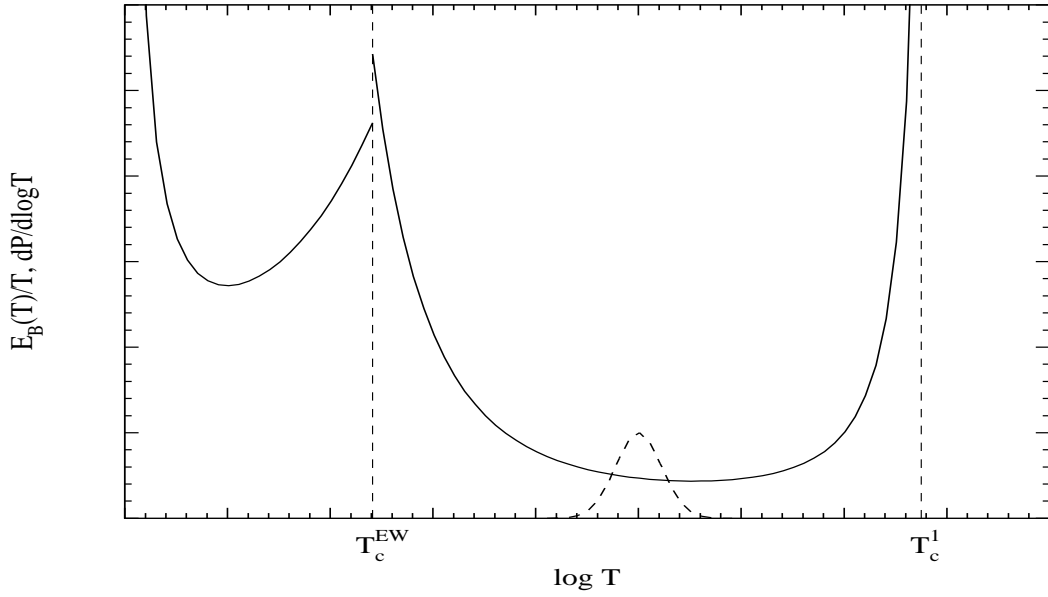


Fig. 10: Ratio of the critical bubble energy to the temperature (solid line) and differential probability for bubble nucleation (dashed) as a function of temperature. T_c^{EW} and T_c^1 are the two critical temperatures.

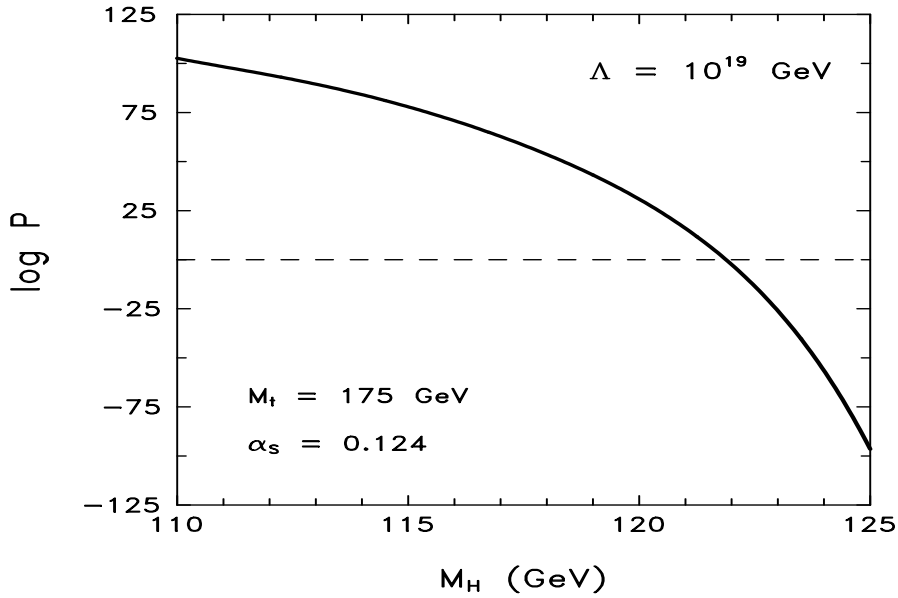


Fig. 11: Logarithm of the total probability of decay to the true vacuum as a function of M_h for $M_t = 175$ GeV. The point where the curve roughly crosses the dashed line gives the metastability bound.

Then, for fixed M_t the probability P of thermal decay to the true vacuum can be computed as a function of M_h . One example is shown in fig. 11 for $M_t = 175 \text{ GeV}$. Note the vast range of variation of P when M_h is changed by a few GeV . Actually this is due to the exponential sensitivity of the decay rate to E_B and then to the shape of the effective potential. From fig. 11 we can derive the so called metastability bound for $M_t = 175 \text{ GeV}$: below $\sim 122 \text{ GeV}$ P is very large and the vacuum decays quickly while for values above that, P is exponentially small and the electroweak vacuum, if metastable, is sufficiently long lived. The critical value $P = 1$ can be taken to compute the critical mass but as is clear from the figure the bound is insensitive to the exact value chosen for the critical probability [provided is very roughly $\mathcal{O}(1)$].

The metastability bounds would depend also on the cut-off scale Λ where new physics is expected to appear[†]. By definition we can compute reliably the effective potential at field values lower than Λ and temperatures lower than $T_\Lambda \sim \Lambda$. The integrated probability that should be required to be less than $\mathcal{O}(1)$ is then (5.2) with this temperature cut-off implemented

$$P(T_\Lambda) = \int_0^{T_\Lambda} dP(T').$$

For some fixed values of M_t and M_h , the condition $P(T_\Lambda) = 1$ gives T_Λ . The profile of the critical bubble at that temperature can be calculated and in particular the value of the field at the center of the bubble $\phi_B(0)$ obtained. To avoid the decay of the electroweak vacuum for this choice of parameters, new physics should modify the effective potential at values of the field of the order $\phi_B(0)$, i.e. new physics should appear at $\Lambda = \phi_B(0)$.

The numerical results for the metastability bounds are shown in fig. 12 for two values of Λ : 10^{19} GeV (three upper curves) and 10 TeV (three lower curves). For a given Λ the (M_t, M_h) plane gets divided in four different regions. Above the long dashed line the electroweak vacuum is absolutely stable, while below it is only metastable: there is a deeper non-standard minimum developing below Λ . Between the absolute stability lower bound and the solid line the metastable electroweak vacuum is long lived and acceptable. Below the solid line however, it would have decayed by thermal excitations in the early Universe. The short dashed line indicates the metastability bound for quantum tunneling at zero T. For $\Lambda = 10^{19} \text{ GeV}$ the lower metastability bound on the Higgs mass is (for $\alpha_s = 0.118$)

$$M_h(\text{GeV}) > 2.306[M_t(\text{GeV}) - 180] + 138.$$

The implications of these bounds for the existence of new physics beyond the Standard Model are discussed in the next and last section.

[†] Again the precise meaning of this scale is provided by the calculation itself as the scale at which the effect of new physics should affect the finite temperature potential in a way suitable of modifying the decay rates.

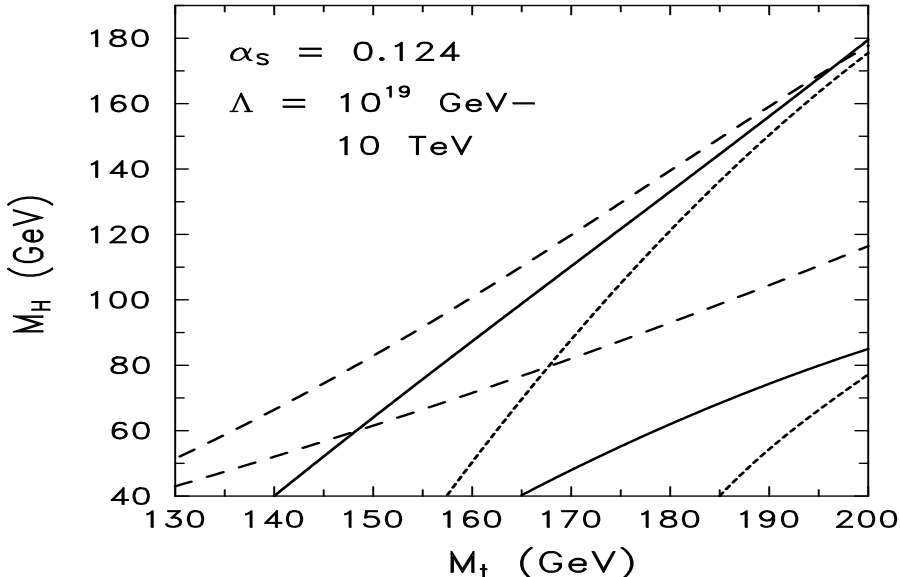


Fig. 12: Lower bounds on the Higgs mass for $\Lambda = 10^{19} \text{ GeV}$ (upper set) and $\Lambda = 10 \text{ TeV}$ (lower set). Long dashed curves give the absolute stability bound, short dashed the metastability bound for quantum tunneling and solid for thermal tunneling in the hot early Universe.

6. Implications

The most important implication of the *lower* bounds on the Higgs mass derived in section 5 is that the measurement of M_h may provide an *upper* bound on the scale Λ of new physics. For this to be true, the top mass should be heavy enough so that some instability would appear in the Standard Model potential if the new physics were not present. Numerically the requirement is (all masses in GeV)

$$M_t > \frac{M_h}{2.25} + 123 \text{ GeV}. \quad (6.1)$$

(This is obtained from the metastability bound for $\Lambda = 10^{19} \text{ GeV}$). In particular, for Higgs masses above the experimental limit $\sim 65 \text{ GeV}$ the top quark should be heavier than $\sim 152 \text{ GeV}$, which is the case. Similarly, (6.1) also tells that, unless $M_t < 160 \text{ GeV}$, the discovery of a Higgs boson by LEP II would imply that the Standard Model cannot be valid up to the Planck Scale.

Moreover, in most of the parameter space, the scale below which new physics should enter is much smaller than M_{Pl} . Consider for example fig. 13 where metastability bounds for different top masses are plotted as a function of the scale Λ . Suppose now that LEP II finds a 90 GeV Higgs boson. Then, if $M_t > 170 \text{ GeV}$, we can

read from the figure that new physics should appear below $\Lambda \sim 10^6 \text{ GeV}$. Otherwise, the Standard Model potential would be unstable and our vacuum would have decayed long ago.

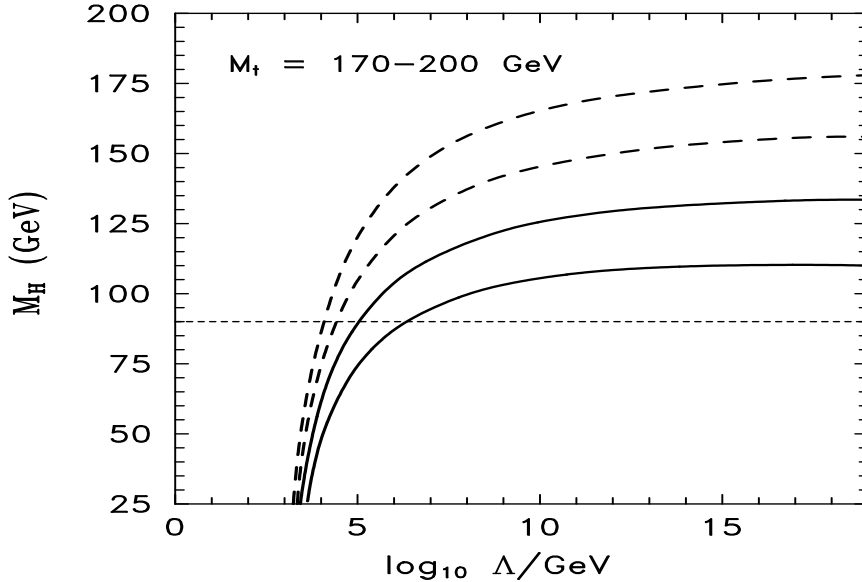


Fig. 13: Metastability bounds on the SM Higgs boson mass as a function of the cut-off Λ for the indicated values of the top mass (lower curve for lower M_t). The horizontal line indicates roughly the reach of LEP II.

Of course, the new physics should be such that this instability is cured. For example, a heavy fourth generation would make the effective potential even more unstable (a new large Yukawa coupling would add to the destabilization effect of the top quark). Then, this kind of stability analysis can in fact be used to constrain such extensions of the Standard Model (see A. Novikov's contribution to these proceedings). As a prime example of new physics that would go in the good direction we can consider the Minimal Supersymmetric Standard Model. In the MSSM, it turns out that the running of the quartic Higgs coupling is no longer dominated by the top Yukawa coupling. The effect of top quark loops is compensated by stops, the supersymmetric partners of the top. The relevant diagrams are shown in fig. 14 . In fact, quartic Higgs couplings in the MSSM run like gauge couplings. This effect is schematically depicted in fig. 14 . Below the supersymmetric scale Λ the quartic Higgs coupling decreases steeply due to top loop effects. But once the supersymmetric threshold is crossed, all supersymmetric particles influence the running of λ with the effect of Yukawas cancelling and leaving just the gauge renormalization. The figure then shows how the presence of the supersymmetric threshold prevents λ to become negative and makes it rise again, thus stabilizing the potential.

In the framework of the MSSM as model for new physics, it is then tempting to try and put an upper bound on the supersymmetric scale by using metastability arguments. Unfortunately, as is shown already in fig. 13, metastability bounds cannot compete with simple naturalness criteria that require $\Lambda_{SUSY} < \mathcal{O}(1) TeV$.

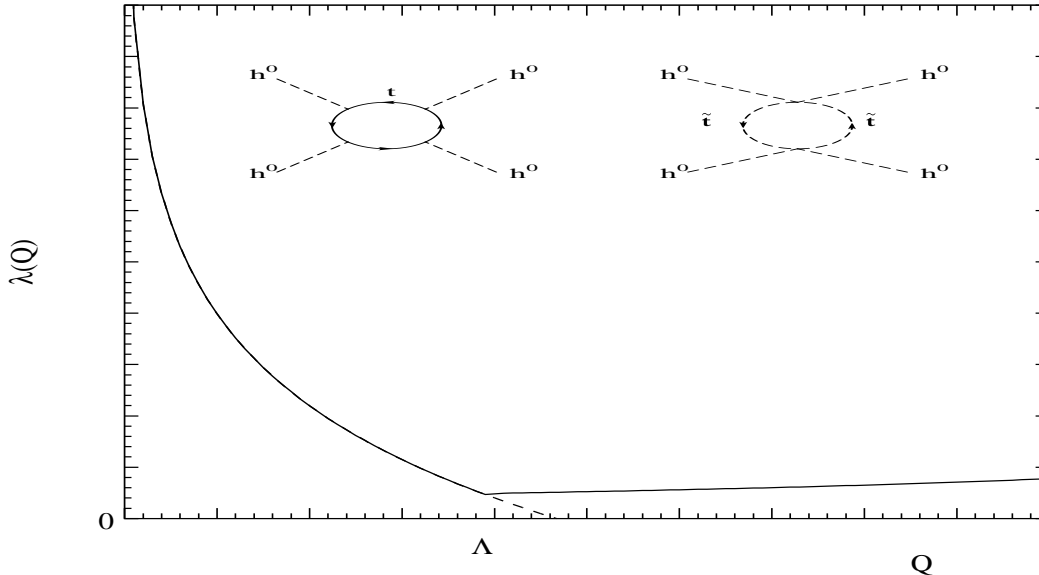


Fig. 14: Schematic running of the quartic Higgs coupling below and above the supersymmetric threshold with the relevant diagrams indicated. The pair (M_t, M_h) is chosen to lie in the instability region.

Nevertheless, useful information can be extracted from the confrontation of the theoretical expectations for Higgs masses in the Standard Model and the MSSM. In fig. 15 we plot (steepest curve) the less restrictive metastability bound for the SM Higgs mass, choosing $\Lambda = 10^{19} GeV$, i.e. assuming validity of the model up to the Planck scale. Superimposed in the same plot it is shown the absolute upper bound on the lightest Higgs mass in the MSSM for $\Lambda_{SUSY} = 1 TeV$ (more or less the limit from naturalness). In both curves the uncertainty caused by α_S in the range indicated is reflected in the dashed curves.

The (M_t, M_h) plane gets divided into four different zones. The experimental determination of the zone actually realized is of great interest. If the Higgs boson is found in the upper left region it would be compatible with the SM but it would be too heavy for the MSSM (remember that we are talking about a neutral Higgs boson with properties similar to the SM one). Alternatively, if it is the lower right area the one chosen by nature, then the Higgs mass would be too low for the pure SM and new physics should appear below the Planck mass. This new physics could well be in the form of the MSSM, and in that region the mass of the Higgs is compatible

with that hypothesis. Finally, the region in the lower left corner is compatible with the SM and MSSM while the upper right corner is incompatible with both.

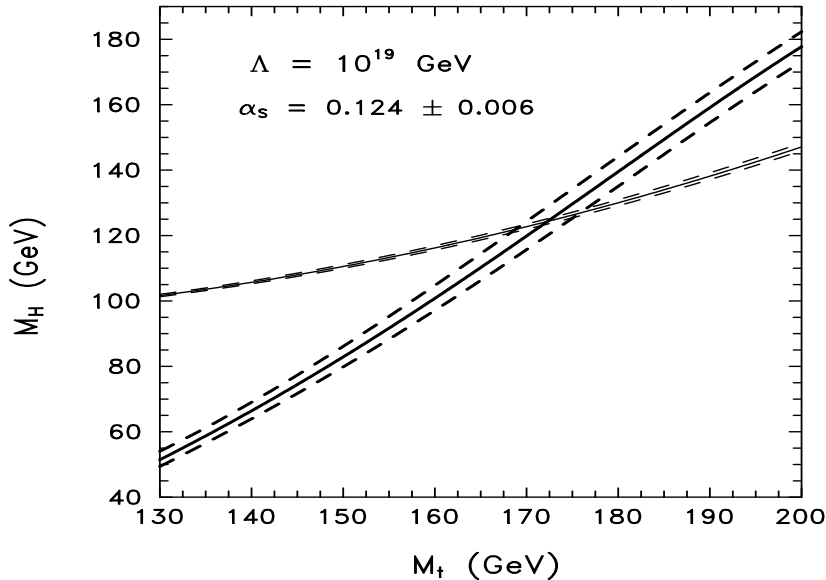


Fig. 15: Absolute lower metastability bound on the SM Higgs mass with $\Lambda = 10^{19} \text{ GeV}$ (steepest curves) and absolute upper bound on the lightest Higgs mass in the MSSM with $M_S = 1 \text{ TeV}$ and maximal stop mixing effect. Dashed lines show the variation when α_s is changed in the indicated range.

So, at least in some regions of parameter space, we may be able to distinguish indirectly between the lightest MSSM Higgs boson in the decoupling SUSY limit and the SM Higgs, which is a very difficult task experimentally. In any case it is remarkable that the detection of a Higgs boson, the last missing ingredient of the Standard Model, can already provide information against the pure SM and point towards the need of new physics at some scale well below the Planck scale.

I would like to thank Marcela Carena, Alberto Casas, Denis Comelli, Mariano Quirós, Antonio Riotto and Carlos Wagner for fruitful and enjoyable collaborations on some of the topics covered here. I also express my gratitude to the organizers of the school for their kind invitation to lecture and their warm hospitality and to all the participants for contributing to a most charming atmosphere. This work was supported by the Alexander-von-Humboldt Foundation.

7. References

7.1 Section 2

The bounds presented in Section 2 were derived in the following references:

- Langacker, P. and Weldon, H.A., *Phys. Rev. Lett.* **52**, 1377 (1984); Weldon, H.A., *Phys. Lett.* **B146**, 59 (1984).
- Comelli, D. and Espinosa, J.R., DESY Preprint to appear.

For analytical and numerical bounds on the lightest Higgs boson in general supersymmetric models see:

- Espinosa, J.R. and Quirós, M., *Phys. Lett.* **B302**, 51 (1993); *Phys. Lett.* **B279**, 92 (1992); Espinosa, J.R., *Phys. Lett.* **B353**, 243 (1995); Kane, G., Kolda, C. and Wells, J.D., *Phys. Rev. Lett.* **70**, 2686 (1993).

A nice example of the decoupling limit in multidoublet Higgs models, with all Higgses heavy but one ‘true’ light Higgs boson, is studied in

- Georgi, H. and Nanopoulos, D.V., *Phys. Lett.* **82B**, 95 (1979).

For a rather complete analysis of the decoupling limit in multi Higgs model see

- Haber, H.E. and Nir, Y., *Nucl. Phys.* **B335**, 363 (1990).

The analysis of Higgs production in the presence of gauge singlets is based on

- Kamoshita, J., Okada, Y. and Tanaka, M., *Phys. Lett.* **B328**, 67 (1994).

7.2 Section 3

For an introduction to the MSSM see e.g. Kazakov’s lectures at this school.

The important effect of radiative corrections in the mass of the lightest Higgs boson in the MSSM was put forward in

- Okada, Y., Yamaguchi, M. and Yanagida, T., *Prog. Theor. Phys.* **85**, 1 (1991); *Phys. Lett.* **B262**, 54 (1991); Haber, H.E. and Hempfling, R. *Phys. Rev. Lett.* **66**, 1815 (1991); Ellis, J., Ridolfi, G., and Zwirner, F., *Phys. Lett.* **B257** 83 (1991); *ibid.* **B262**, 477 (1991); Barbieri, R., Frigeni, M. and Caravaglios, F., *ibid.* **B258**, 167 (1991).

The NTLL calculation of the Higgs boson mass described in the text is in

- Casas, J.A., Espinosa, J.R., Quirós, M. and Riotto, A. *Nucl. Phys.* **B355**, 3 (1995).

Complimentary work can be found in

- Hempfling, R. and Hoang, H., *Phys. Lett.* **B331**, 99 (1994); Kodaira, J., Yasui, Y. and Sasaki, K., *Phys. Rev.* **D50**, 7035 (1994), Haber, H.E., Hempfling, R. and Hoang, H., Preprint CERN-TH/95-216 to appear.

For a good introduction to the use of effective theories see

- Cohen, A.G., in Proceedings of TASI-93, World Scientific, 1994.

Analytical formulas for the MSSM Higgs spectrum that include the most important loop corrections are worked out in

- Carena, M., Espinosa, J.R., Quirós, M. and Wagner, C., *Phys. Lett.* **B355**, 209 (1995); Carena, M., Quirós, M. and Wagner, C., *Nucl. Phys.* **B461**, 407 (1996).

The effective theory below the SUSY scale in the case of low m_A is studied (with particular attention to the mass of the lightest Higgs) in the nice paper

- Haber, H.E. and Hempfling, R., *Phys. Rev.* **D48**, 4280 (1993).

7.3 Section 4

For a review on the Higgs potential, see

- Sher, M., *Phys. Rep.* **179**, 274 (1989).

Lower stability bounds on the SM Higgs mass were originally studied in

- Krasnikov, N.V. *Yadern. Fiz.* **28**, 549 (1978); Politzer, H.D. and Wolfram, S., *Phys. Lett.* **82B**, 242 (1979); Hung, P.Q., *Phys. Rev. Lett.* **42**, 873 (1979); Cabibbo, N., Maiani, L., Parisi, A. and Petronzio, R., *Nucl. Phys.* **B158**, 295 (1979).

For more recent improvements see

- Lindner, M., *Z. Phys.* **C31**, 295 (1986); Lindner, M., Sher, M. and Zaglauer, H.W., *Phys. Lett.* **B228**, 139 (1989); Sher, M., *Phys. Lett.* **B317**, 159 (1993); *ibid.* **B331**, 448 (1994); Ford, C. et al., *Nucl. Phys.* **B395**, 17 (1993).

The calculation of the SM Higgs stability bound including next-to-leading log corrections as described in the text is in

- Casas, J.A., Espinosa, J.R. and Quirós, M., *Phys. Lett.* **B342**, 171 (1995); and Preprint DESY 96-021 [hep-ph/9603227] to appear in *Phys. Lett.* **B**.

For an independent analysis along similar lines see

- Altarelli, G. and Isidori, I., *Phys. Lett.* **B337**, 141 (1994).

For studies of the renormalization-group improved effective potential see

- Coleman, S. and Weinberg, E., *Phys. Rev.* **D7**, 1888 (1973).
- Kastening, B., *Phys. Lett.* **B283**, 287 (1992); Ford, C. et al., *Nucl. Phys.* **B395**, 17 (1993); Bando, M., et al., *Phys. Lett.* **B301**, 83 (1993); *Prog. Theor. Phys.* **90**, 405 (1993).

7.4 Section 5

For an introduction to the decay of metastable vacuum states see e.g.

- Voloshin, M.B., Lecture at International School of Subnuclear Physics, Erice 1995.

Lower metastability bounds on the SM Higgs mass were obtained in:

- Anderson, G., *Phys. Lett.* **B243**, 265 (1990); Arnold, P. and Vokos, S., *Phys. Rev.* **D44**, 3620 (1991).

The next-to-leading log bound is presented in

- Espinosa, J.R. and Quirós, M., *Phys. Lett.* **B35**, 257 (1995).

7.5 Section 6

The interplay between the SM lower bound on the Higgs mass and the upper bound for the lightest Higgs boson in the MSSM was considered by

- Krasnikov, N.V. and Pokorski, S., *Phys. Lett.* **B288**, 184 (1992); Díaz, M.A., ter Veldhuis, T.A. and Weiler, T.J., *Phys. Rev. Lett.* **74**, 2876 (1995).

The analysis with the most refined bounds is presented in

- Casas, J.A., Espinosa, J.R. and Quirós, M., *Phys. Lett.* **B342**, 171 (1995).